JASA ARTICLE

Acoustic radiation force exerted by progressive waves on subwavelength inhomogeneous scatterers

Chirag A. Gokani,[1,2,a)] Thomas S. Jerome,[1] Michael R. Haberman,[1,2] and Mark F. Hamilton[1,2]
[1]*Applied Research Laboratories, The University of Texas at Austin, Austin, Texas 78766-9767, USA*
[2]*Walker Department of Mechanical Engineering, The University of Texas at Austin, Austin, Texas 78712-1063, USA*

ABSTRACT:
The acoustic radiation force exerted by plane progressive waves with wavenumber k on a scatterer of characteristic size a is calculated in the Born approximation using Westervelt's far-field integral [J. Acoust. Soc. Am. **29**, 26–29 (1957), Eq. (2)]. In the subwavelength limit $ka \ll 1$ of the Born approximation, closed-form analytical expressions for the radiation force are obtained in terms of acoustic polarizabilities, which represent the response of the scatterer to dipole order. For subwavelength scatterers whose relative compressibility and density are even functions about their centroid, Gor'kov's $O[(ka)^4]$ force [Sov. Phys. Dokl. **6**, 773–775 (1962), Eq. (10)] is recovered, whereas the radiation force on scatterers characterized by odd distributions is $O[(ka)^6]$. Radiation forces on homogeneous and inhomogeneous spheres and cubes are considered as examples, for which the analytical expressions agree with solutions based on spherical wave expansions and Fourier transforms for $ka \lesssim 0.8$. The present work complements the volume integral obtained by Jerome and Hamilton [J. Acoust. Soc. Am. **150**, 3417–3427 (2021), Eq. (16)] for the radiation force exerted by standing waves in the subwavelength limit of the Born approximation.
 https://doi.org/10.1121/10.0043002

(Received 29 October 2025; revised 29 January 2026; accepted 23 February 2026; published online 3 April 2026)
[Editor: Philip L. Marston] Pages: 3030–3047

I. INTRODUCTION

Radiation force is the time-averaged force exerted by waves on scatterers. The force arises because of momentum conservation at quadratic order in the solution of the wave equation.[1] Both progressive and standing waves are capable of exerting radiation forces, but the forces differ in their dependence on both position and frequency.[2] For plane waves, the differences can be understood qualitatively by noting that progressive waves carry time-averaged intensity, whereas standing waves do not. Conversely, standing waves form time-averaged gradients of energy, whereas progressive waves do not.

Perhaps the first observation of radiation force in nature was that exerted by progressive waves of sunlight on the tails of comets. Chinese astronomers noted that comet tails point away from the Sun in 66 AD,[3] when the appearance of Halley's Comet was first accurately recorded.[4] Tycho Brahe wrote that the Great Comet of 1577 "had its tail turned directly away from the Sun, as all other comets, those observed many years ago by Regiomontanus, Apian, Gemma Frisius, and Fracastoro, have also done,"[5] indicating that the phenomenon was known in the West as early as Regiomontanus's observation of the Great Comet of 1472.[6] Johannes Kepler, who witnessed the Great Comet of 1577 at the age of six,[7] concluded following his observations of Halley's Comet in 1607 and the Great Comet of 1618 that "a comet's tail is formed by matter that the Sun's rays chase through their impulses outside the comet's body."[8,9] According to Beyer, Euler explained the phenomenon by analogy to acoustics, noting that "a sound vigorously excites not only a vibratory motion in the air particles" but also causes "a real motion in small, very light dust particles which tumble in the air."[10] Forces due to progressive electromagnetic waves were subsequently described mathematically by Maxwell[11] and Poynting,[12,13] and the analogous acoustical problem was described by Rayleigh.[14]

Interest in radiation forces exerted by standing waves began with Kundt's report of a powder in a tube accumulating near the nodes of a standing acoustic wave field.[15] Rayleigh[16] and Brillouin[17] calculated forces exerted by oscillations of a pendulum and standing waves on a string before considering the more involved acoustical problem, as reviewed by Beyer.[10] A discussion of the history, calculation, and applications of forces exerted by standing acoustic waves is provided by Bruus.[18]

Current interest in radiation forces exerted by both standing and progressive waves is largely motivated by acoustofluidics.[19–21] Contributions by Mishra *et al.*,[22] Jerome *et al.*,[23] Lima and Silva,[24] and Abraham-Ekeroth *et al.*[25] have facilitated the calculation of forces exerted by standing waves on asymmetric[26] and/or inhomogeneous[27] objects. Although forces exerted by progressive waves have been considered for the purpose of particle manipulation[28–32] and transport over long distances,[33–35] closed-form expressions for such forces on asymmetric and/or inhomogeneous objects remain

a)Email: chiragokani@utexas.edu

https://doi.org/10.1121/10.0043002

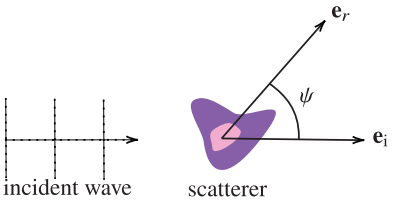

FIG. 1. Spherical radial unit vector $\mathbf{e}_r$, incident wave unit vector $\mathbf{e}_i$, and scattering angle $\psi = \arccos(\mathbf{e}_i \cdot \mathbf{e}_r)$ shown with respect to the incident plane progressive wave and scatterer.

unavailable.[36,37] The goal of the present work is to obtain analytical expressions for the force exerted by progressive waves analogous to those obtained by Jerome *et al.* for standing waves.[23,27]

Jerome *et al.* showed that the radiation force exerted by a standing wave on a scatterer can be obtained by integrating differential radiation forces over the volume of a scatterer.[23] Although radiation forces are proportional to the squares of the total acoustic fields and therefore do not generally superpose,[2] the superposition principle underlying the integration is justified in the Born approximation, which neglects the effects of multiple scattering.[38] The Born approximation itself requires that the scattered field be much weaker than the incident field, a condition that is satisfied if the relative phase shift is small compared with an incident wave that misses the scatterer. The same conditions underlie the Rayleigh-Gans approximation in electromagnetic scattering.[39] The Born approximation is therefore satisfied if contrasts between the material properties of the scatterer and background medium are much smaller than unity,[40] and if the products of the relative contrasts and the characteristic size a of the scatterer are much smaller than the wavelength $2\pi/k$.[38,39,41] In practice, the forces calculated by Jerome *et al.* converge to exact solutions for $ka \lesssim 1$, with a number of examples transcending that limit for sufficiently weak material contrasts [e.g., Ref. 23, Fig. 1(a)].

The integral for the radiation force is calculated by Jerome and Hamilton by noting that in standing waves, the differential force is proportional to the scatterer's differential volume $\mathrm{d}V_s$.[27] However, the approach does not apply to progressive waves, for which the differential force is proportional to $(\mathrm{d}V_s)^2$, prohibiting integration over a scatterer's finite volume.[23] To calculate forces exerted by progressive waves, the present work makes approximations on the same order as those made by Jerome *et al.*, but at different stages of the calculation. The Born and subwavelength approximations are invoked not as justifications to superpose differential radiation forces but rather as a means to solve the linear scattering problem.

The radiation force parallel to the unit vector $\mathbf{e}_i$ indicating the direction of the incident wave is obtained by inserting the directivity Φ of the scattered wave into Westervelt's integral,[42,43]

$$F_{\parallel} = \frac{p_0^2}{2\rho_0 c_0^2} \oint |\Phi|^2 (1 - \mathbf{e}_i \cdot \mathbf{e}_r)\, \mathrm{d}\Omega, \tag{1}$$

where p_0 is the incident pressure amplitude, ρ_0 is the density of the background fluid, $\mathbf{e}_r$ is the spherical radial unit vector, and $\mathrm{d}\Omega$ is the differential solid angle, e.g., $\sin\theta\, \mathrm{d}\theta\, \mathrm{d}\phi$ in spherical coordinates, where θ and ϕ are the spherical polar and azimuthal angles, respectively. The relationship between $\mathbf{e}_i$ and $\mathbf{e}_r$ is shown in Fig. 1 with respect to the incident progressive wave and scatterer. The speed of sound c_0 in the background fluid equals $1/\sqrt{\beta_0 \rho_0}$, where β_0 is the compressibility of the fluid.

Expressions for the directivity Φ appearing in Eq. (1) are obtained by appealing to the Born and subwavelength approximations in Secs. II and III, respectively. Equation (1) is evaluated for homogeneous and inhomogeneous spheres and cubes in Sec. IV, in which the resulting analytical expressions for $F_{\parallel}$ are compared with solutions in terms of spherical wave expansions and Fourier transforms. Westervelt's[43] 1957 derivation of Eq. (1) is reviewed in Appendix A, where the final step of the derivation is clarified by appealing to energy conservation, and a qualitative derivation of Eq. (1) in terms of the scattering cross section is provided by van de Hulst.[39] Although Eq. (1) is applicable to lossless scattering, the effect of absorption is discussed by Westervelt[43] and Zhang and Marston.[44] An alternative perspective on Eq. (1) is provided in the framework of momentum by Zhang and Marston in terms of phase shifts.[45]

II. FAR FIELD OF BORN APPROXIMATION

The propagation of time-harmonic acoustic waves in an inhomogeneous medium is described by[40]

$$\nabla^2 \tilde{p} + k^2 \tilde{p} = -k^2 \gamma_\beta \tilde{p} + \nabla \cdot (\gamma_\rho \nabla \tilde{p}), \tag{2}$$

where the pressure field is related to $\tilde{p}$ by

$$p(\mathbf{r}, t) = \mathrm{Re}\left[\tilde{p}(\mathbf{r}) e^{-i\omega t}\right], \tag{3}$$

and $\mathbf{r}$ is the position vector, t is time, and ω is the angular frequency kc_0, where k is the wavenumber. The functions γ_β and γ_ρ in Eq. (2) are Morse and Ingard's[40] dimensionless contrast factors

$$\gamma_\beta(\mathbf{r}) = \frac{\beta_s(\mathbf{r})}{\beta_0} - 1, \qquad \gamma_\rho(\mathbf{r}) = 1 - \frac{\rho_0}{\rho_s(\mathbf{r})}, \tag{4}$$

where β_s and ρ_s are the scatterer's compressibility and density as functions of position within the scatterer, respectively. Equations (4) are defined such that $\gamma_\beta = \gamma_\rho = 0$ outside the region occupied by the scatterer.

The integral form of the inhomogeneous Helmholtz equation given by Eq. (2) is

$$\tilde{p}(\mathbf{r}) = \tilde{p}_i(\mathbf{r}) + \tilde{p}_s(\mathbf{r}), \tag{5}$$

where $\tilde{p}_i(\mathbf{r})$ is the incident wave, and[40]

$$\tilde{p}_s(\mathbf{r}) = \int \Big[k^2 \gamma_\beta(\mathbf{r}_s)\tilde{p}(\mathbf{r}_s) g(\mathbf{r}|\mathbf{r}_s) + \gamma_\rho(\mathbf{r}_s)\, \boldsymbol{\nabla}_s \tilde{p}(\mathbf{r}_s) \cdot \boldsymbol{\nabla}_s g(\mathbf{r}|\mathbf{r}_s) \Big] \mathrm{d}V_s \tag{6}$$

is the scattered wave, and

$$g(\mathbf{r}|\mathbf{r}_s) = \frac{e^{ik|\mathbf{r}-\mathbf{r}_s|}}{4\pi|\mathbf{r}-\mathbf{r}_s|} \tag{7}$$

is the free-space Green's function of the Helmholtz equation. Although the domain of integration of Eq. (6) is over all space, the evaluation of Eq. (6) amounts to a volume integral over the body of the scatterer because γ_β and γ_ρ vanish beyond the scatterer's boundary. Equations (2) and (6) are given by Eqs. (8.1.12) and (8.1.13) of Ref. 40, respectively, the derivations of which are reviewed in Appendix B.

The relationship between the integration coordinate $\mathbf{r}_s$ and the observation coordinate $\mathbf{r}$ with respect to the origin

$$\mathbf{0} = \frac{\int_{V_s} \mathbf{r}_s \, \mathrm{d}V_s}{\int_{V_s} \mathrm{d}V_s} \tag{8}$$

is shown in Fig. 2, where V_s denotes the region occupied by the scatterer. The identification of the origin as the centroid given by Eq. (8), as opposed to the center of mass, is consistent with previous scattering formulations[23,27,46] and is discussed further in Sec. III.

For an incident plane progressive wave $\tilde{p}_i = p_0 e^{i\mathbf{k}_i\cdot\mathbf{r}}$, where $\mathbf{k}_i = k\mathbf{e}_i$ is the incident wave vector, the scattered wave given by Eq. (6) reduces in the far field of the Born approximation to

$$\tilde{p}_s(\mathbf{r}) = p_0 \frac{e^{ikr}}{r} \Phi(\mathbf{k}_s), \tag{9}$$

where $\mathbf{k}_s = k\mathbf{e}_r$ is the scattered wave vector and $r = |\mathbf{r}|$. Equation (9) represents a spherically spreading scattered wave with a directivity given by Eq. (8.1.14) of Ref. 40:

$$\Phi(\mathbf{k}_s) = \frac{k^2}{4\pi} \Big[\mathcal{F}_{3D}\Big\{ \gamma_\beta(\mathbf{r}_s) e^{i\mathbf{k}_i\cdot\mathbf{r}_s} \Big\} + \mathcal{F}_{3D}\Big\{ \gamma_\rho(\mathbf{r}_s) e^{i\mathbf{k}_i\cdot\mathbf{r}_s} \Big\} \mathbf{e}_i \cdot \mathbf{e}_r \Big]. \tag{10}$$

The three-dimensional Fourier transform pair is defined by

$$\mathcal{F}_{3D}\{f(\mathbf{r}_s)\} = \int f(\mathbf{r}_s) e^{-i\mathbf{k}_s\cdot\mathbf{r}_s} \mathrm{d}V_s, \tag{11}$$

$$\mathcal{F}^{-1}_{3D}\{F(\mathbf{k}_s)\} = \frac{1}{8\pi^3} \int F(\mathbf{k}_s) e^{i\mathbf{k}_s\cdot\mathbf{r}_s} \mathrm{d}W_s, \tag{12}$$

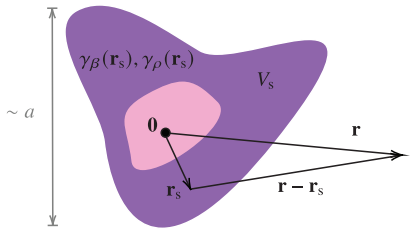

FIG. 2. Geometry of scatterer of characteristic size a, volume V_s, and material properties given by Eq. (4). The origin $\mathbf{0}$ is defined by Eq. (8) to be the centroid of the scatterer.

and $\mathrm{d}V_s$ and $\mathrm{d}W_s$ are differential volume elements in position and wavenumber space, respectively, where the domains of integration are infinite. Equations (9) and (10) follow immediately from Eq. (6) upon noting that Eq. (7) and its gradient are given approximately by Eqs. (23) in the far field.

Evaluation of Westervelt's integral given by Eq. (1) for Φ given by Eq. (10) results in the Born approximation of the radiation force exerted by plane progressive waves on scatterers of arbitrary size with respect to a wavelength. Although Westervelt's integral in combination with Eq. (10) is used simply to benchmark the subwavelength limit of the Born approximation in Sec. IV, the combination is valuable in its own right because its evaluation is considerably simpler than calculating radiation forces using partial wave expansions or the finite element method.[36,37,47] The study of how the Born approximation beyond the subwavelength limit compares to other methods falls beyond the scope of the present work but may be pursued in the future.

The far-field approximation leading to the scattered pressure given by Eq. (9) is based on the assumption that the spherical radial field coordinate r is much larger than the characteristic scatterer size a, allowing for the phase $k|\mathbf{r}-\mathbf{r}_s|$ of the Green's function to be approximated as $k(r - \mathbf{e}_r\cdot\mathbf{r}_s + r_s^2/2r)$, where $k|\mathbf{r}_s| = kr_s = O(ka)$. Thus for $r/a \gg ka$, one obtains

$$k|\mathbf{r}-\mathbf{r}_s| = k(r - \mathbf{e}_r\cdot\mathbf{r}_s). \tag{13}$$

The far-field approximation is therefore always valid in the study of scattering for $ka \ll 1$ considered in Sec. III because the inequality $r/a \gg ka$ is satisfied for $r > a$. The far-field approximation is also on equal footing with Westervelt's integral, which requires that the scattered intensity be proportional to r^{-2}, as can be seen in Eq. (A13). The far-field approximation as it pertains to the calculation of radiation force does "not introduce any approximation…in the idealized case of loss-less media."[48]

Conditions for the validity of the Born approximation leading to Φ given by Eq. (10) are more subtle. As stated in Sec. I, although weak material contrast ($|\gamma_\beta|, |\gamma_\rho| \ll 1$) often satisfies the Born approximation, weak scattering may also be achieved if the scatterer is sufficiently small ($ka \ll 1$), provided that the frequency of the incident wave is not in the proximity of the resonance frequency of the scatterer.[49–51] A very small scatterer with large material contrast may therefore

https://doi.org/10.1121/10.0043002

satisfy the Born approximation as well as a much larger scatterer with sufficiently small material contrast, as discussed in Sec. IV. The interrelated nature of the low-contrast and low-ka conditions is summarized by Pierce, who denotes $\Delta_1 = 1 - \rho_0/\rho(\mathbf{r}) = \gamma_\rho$ and $\Delta_2 = 1 - \beta(\mathbf{r})/\beta_0 = -\gamma_\beta$:[38]

> Although [the Born approximation] requires in general that the scattered wave in the steady state be much weaker than the incident wave wherever the dominant inhomogeneities occur, no simple criteria involving magnitudes of Δ_1 and Δ_2 establish the upper limits of the approximation's validity. It should, however, yield a good estimate of the scattered field if $|\Delta_1| \ll 1$ and $|\Delta_2| \ll 1$, and if the path integrals of both $k|\Delta_1|$ and $k|\Delta_2|$ are small compared with unity.

The interdependence between low contrast and long wavelength and its effect on the validity of the Born approximation is evident in Fig. 1(a) of Jerome *et al.*,[23] in which the contrast is sufficiently weak that the radiation force predicted by the Born approximation agrees with the full expression of the force based on spherical wave expansions[52] for $ka = O(10)$. A similar interdependence is reported in Refs. 39, 41, and 53, and a more detailed discussion on how the validity of the Born approximation depends on frequency is provided in Ref. 54. For the present work, it suffices to note that Westervelt's integral in terms of Φ given by Eq. (10) is accurate for $ka > O(1)$ only if the sound speed within the scatterer is sufficiently close to that of the background medium such that the cumulative error due to propagation at a different phase speed within the scatterer can be neglected.

III. SUBWAVELENGTH LIMIT

The present section is devoted to obtaining the subwavelength limit of Φ given by Eq. (10), for which the Born approximation is more broadly satisfied, and for which evaluation of Westervelt's integral yields closed-form analytical expressions. Begin by noting that $|\mathbf{k}_\mathrm{i}| = |\mathbf{k}_\mathrm{s}| = k$ and $|\mathbf{r}_\mathrm{s}| = O(a)$. The products $\mathbf{k}_\mathrm{i} \cdot \mathbf{r}_\mathrm{s}$ and $\mathbf{k}_\mathrm{s} \cdot \mathbf{r}_\mathrm{s}$ are therefore $O(ka)$. Assuming that $ka \ll 1$ therefore warrants the expansion of the complex exponentials in Eqs. (9)–(12) to linear order as

$$e^{i\mathbf{k}_\mathrm{i}\cdot\mathbf{r}_\mathrm{s}} \simeq 1 + i\mathbf{k}_\mathrm{i} \cdot \mathbf{r}_\mathrm{s}, \tag{14}$$

$$e^{-i\mathbf{k}_\mathrm{s}\cdot\mathbf{r}_\mathrm{s}} \simeq 1 - i\mathbf{k}_\mathrm{s} \cdot \mathbf{r}_\mathrm{s}. \tag{15}$$

Equation (10) in terms of Eqs. (11), (14), and (15) becomes

$$\Phi(\mathbf{k}_\mathrm{s}) = \frac{1}{4\pi}\int\left[k^2\gamma_\beta(\mathbf{r}_\mathrm{s}) + \mathbf{k}_\mathrm{s}\cdot\mathbf{k}_\mathrm{i}\gamma_\rho(\mathbf{r}_\mathrm{s})\right] \times [1 + i(\mathbf{k}_\mathrm{i} - \mathbf{k}_\mathrm{s})\cdot\mathbf{r}_\mathrm{s}]\,\mathrm{d}V_\mathrm{s}, \tag{16}$$

where terms proportional to $(\mathbf{k}_\mathrm{i} \cdot \mathbf{r}_\mathrm{s})(\mathbf{k}_\mathrm{s} \cdot \mathbf{r}_\mathrm{s}) = O[(ka)^2]$ have been neglected.

The retention of the linear terms in Eqs. (14) and (15) restricts the accuracy of the scattered pressure given by Eq. (9) combined with Eq. (16) to dipole order, as can be shown by alternatively expressing Eq. (9) as the pressure field scattered by a point located at the origin $\mathbf{0}$,[55]

$$\tilde{p}_\mathrm{s}(\mathbf{r}) = -k^2\rho_0 c_0^2 m g(\mathbf{r}|\mathbf{0}) + ikc_0\mathbf{d}\cdot\nabla g(\mathbf{r}|\mathbf{0}). \tag{17}$$

The scalar m in Eq. (17) is the monopole strength, and the vector $\mathbf{d}$ is the acoustic dipole moment. Equation (17) is consistent with the dipole-order expansion of Sieck *et al.* given by Eqs. (19) and (20) of Ref. 55, and a derivation of Eq. (17) from first principles is presented in Appendix C in the present work. Although several other conventions of dipole-order expansions appear in the literature,[38,46,56,57] the expansion given by Eq. (17) is conducive to the present study because it can be interpreted as the Born approximation for a point scatterer of the exact scattered field given by Eq. (6). The relationship between Eqs. (6) and (17) is reminiscent of the relationship between the full radiation force exerted by a standing wave on a compressible sphere and its point scattering approximation, given by Eqs. (3) and (6), respectively, of Jerome *et al.*[23] Monopolar and dipolar fields were discussed previously in the context of radiation force by Fan and Zhang,[58] whose analysis is based on the phase-shift-related expressions developed by Zhang and Marston,[45] and by Sepehrirahnama *et al.*,[59–61] whose results are discussed at the end of the present section.

The monopole strength and dipole moment appearing in Eq. (17) are related to the incident pressure and fluid velocity fields by acoustic polarizabilities, which represent the combined influence of the geometry and composition of a scatterer in the long-wavelength limit. The concept of polarizability originated in electromagnetism,[62–64] and an accessible introduction to the use of polarizability in subwavelength electromagnetic scattering is provided on pp. 63–65 of Ref. 39. Polarizability was introduced in acoustics by Senior[65] to describe scattering in the static limit, for which the Helmholtz equation reduces to the Laplace equation. Acoustic polarizabilities have since been discussed in Refs. 38, 55–57, and 59–61, and a recent review of the use of acoustic polarizability in the study of subwavelength scattering is provided by Lawrence.[66] The present work employs the coupled linear equations

$$m = -\beta_0\alpha_\mathrm{m}\tilde{p}_\mathrm{i} - ic_0^{-1}\boldsymbol{\alpha}_\mathrm{c}\cdot\tilde{\mathbf{u}}_\mathrm{i}, \tag{18}$$

$$\mathbf{d} = -ic_0^{-1}\boldsymbol{\alpha}_\mathrm{c}\tilde{p}_\mathrm{i} + \rho_0\underline{\boldsymbol{\alpha}}_\mathrm{d}\cdot\tilde{\mathbf{u}}_\mathrm{i} \tag{19}$$

introduced by Sieck *et al.*,[55] where the volumetric quantities α_m, $\underline{\boldsymbol{\alpha}}_\mathrm{d}$, and $\boldsymbol{\alpha}_\mathrm{c}$ are the monopolar, dipolar, and coupled polarizabilities, respectively. The monopolar polarizability α_m is a scalar that linearly relates a time-harmonic incident pressure field to the monopole strength of the scattered field, as shown in Fig. 3(a). The dipolar polarizability $\underline{\boldsymbol{\alpha}}_\mathrm{d}$ is a rank-2 tensor that relates a time-harmonic incident velocity field to the dipole moment of the

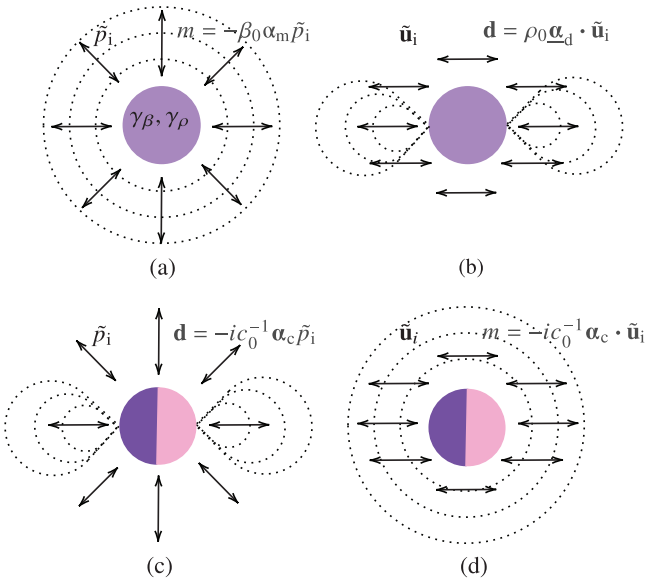

FIG. 3. Field scattered by a homogeneous subwavelength object insonified by a time-harmonic incident (a) pressure field and (b) velocity field, yielding monopole and dipole scattered fields, respectively, proportional to the contrast in material properties and represented by the polarizabilities α_m and $\underline{\boldsymbol{\alpha}}_d$. This is shown in contrast to the field scattered by an inhomogeneous subwavelength scatterer with an antisymmetric property distribution insonified by a time-harmonic incident (c) pressure field and (d) velocity field, yielding dipole and monopole scattered fields, respectively, and represented by the coupled polarizability vector $\boldsymbol{\alpha}_c$.

scattered field, as shown in Fig. 3(b). The coupled polarizability $\boldsymbol{\alpha}_c$ is a vector representing the asymmetry of the scatterer that relates the incident pressure and velocity fields to the dipole moment and monopole strength, respectively, as shown in Figs. 3(c) and 3(d).

Because incident plane waves consist of both time-harmonic pressure and velocity fields,[67] the field scattered by a subwavelength object generally includes contributions from α_m, $\underline{\boldsymbol{\alpha}}_d$, and $\boldsymbol{\alpha}_c$, as shown in Fig. 4. Since the incident field equals $\tilde{p}_i = p_0 e^{i\mathbf{k}_i \cdot \mathbf{r}}$, the incident pressure and velocity fields at $\mathbf{r} = \mathbf{0}$ are

$$\tilde{p}_i = p_0, \qquad \tilde{\mathbf{u}}_i = \mathbf{k}_i p_0 / k \rho_0 c_0, \tag{20}$$

where the second equation is obtained by inserting $\tilde{p}_i$ into the time-harmonic form of the linearized momentum equation $\tilde{\mathbf{u}}_i(\mathbf{r}) = \nabla \tilde{p}_i(\mathbf{r}) / ik\rho_0 c_0$. In terms of Eq. (20), the monopole strength and dipole moment defined by Eqs. (18) and (19) become

$$m = -\beta_0 \alpha_m p_0 - i \boldsymbol{\alpha}_c \cdot \mathbf{k}_i p_0 / k \rho_0 c_0^2, \tag{21}$$

$$\mathbf{d} = -i \boldsymbol{\alpha}_c p_0 / c_0 + \underline{\boldsymbol{\alpha}}_d \cdot \mathbf{k}_i p_0 / k c_0. \tag{22}$$

The far-field limit of the scattered pressure given by Eq. (17) is obtained by noting from Eq. (13) that

$$g(\mathbf{r}|\mathbf{r}_s) \simeq \frac{e^{ikr}}{4\pi r} e^{-i\mathbf{k}_s \cdot \mathbf{r}_s}, \qquad \nabla_s g \simeq -i \mathbf{k}_s g \tag{23}$$

for $r \gg a$, yielding

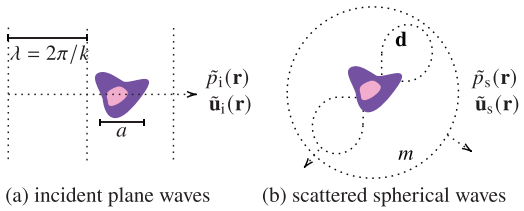

FIG. 4. (a) Incident plane progressive waves consist of both time-harmonic pressure and velocity fields given by $\tilde{p}_i = p_0 e^{i\mathbf{k}_i \cdot \mathbf{r}}$ and $\tilde{\mathbf{u}}_i(\mathbf{r}) = p_0 \mathbf{k}_i e^{i\mathbf{k}_i \cdot \mathbf{r}} / k \rho_0 c_0$, respectively. (b) The monopole, dipole, and coupling polarizabilities defined by Eqs. (18) and (19) therefore contribute to the scattered fields.

$$\tilde{p}_s(\mathbf{r}) = \frac{e^{ikr}}{4\pi r} (-k^2 \rho_0 c_0^2 m + k c_0 \mathbf{d} \cdot \mathbf{k}_s). \tag{24}$$

Insertion of Eqs. (21) and (22) into Eq. (24) and combination with the far field of the scattered pressure given by Eq. (9) yields

$$\Phi(\mathbf{k}_s) = \frac{k^2}{4\pi} \left[\alpha_m + i \boldsymbol{\alpha}_c \cdot (\mathbf{e}_i - \mathbf{e}_r) + \mathbf{e}_r \cdot \underline{\boldsymbol{\alpha}}_d \cdot \mathbf{e}_i \right]. \tag{25}$$

Comparing Eq. (25) with Φ given by Eq. (16) identifies

$$\alpha_m = \int \gamma_\beta(\mathbf{r}_s) \, dV_s, \tag{26}$$

$$\underline{\boldsymbol{\alpha}}_d = \underline{\mathbf{I}} \int \gamma_\rho(\mathbf{r}_s) \, dV_s = \underline{\mathbf{I}} \alpha_d, \tag{27}$$

$$\boldsymbol{\alpha}_c = k \left[\int \gamma_\beta(\mathbf{r}_s) \mathbf{r}_s \, dV_s + \mathbf{e}_i \cdot \mathbf{e}_r \int \gamma_\rho(\mathbf{r}_s) \mathbf{r}_s \, dV_s \right], \tag{28}$$

where $\underline{\mathbf{I}}$ is the identity tensor. The radiation force exerted by plane progressive waves on subwavelength scatterers satisfying the Born approximation is obtained by evaluating Westervelt's integral given by Eq. (1) for

$$|\Phi|^2 = \frac{k^4}{16\pi^2} \{ \alpha_m^2 + 2\alpha_m \alpha_d \cos\psi + \alpha_d^2 \cos^2\psi + [\boldsymbol{\alpha}_c \cdot (\mathbf{e}_i - \mathbf{e}_r)]^2 \}, \tag{29}$$

where $\mathbf{e}_i \cdot \mathbf{e}_r = \cos\psi$, as shown in Fig. 1. In the special case that $\boldsymbol{\alpha}_c = \mathbf{0}$, Westervelt's integral reduces to

$$F_\parallel = \frac{p_0^2}{2\rho_0 c_0^2} \frac{k^4}{4\pi} \left(\alpha_m^2 - \frac{2}{3} \alpha_m \alpha_d + \frac{1}{3} \alpha_d^2 \right), \tag{30}$$

a result that is compared with solutions based on spherical wave expansions and Fourier transforms in Sec. IV. In such cases, perpendicular components of the radiation force vanish, as can be seen by inserting $|\Phi|^2$ given by Eq. (29) for $\boldsymbol{\alpha}_c = \mathbf{0}$ into[43]

$$F_\perp = -\frac{p_0^2}{2\rho_0 c_0^2} \oint |\Phi|^2 \, \mathbf{e}_m \cdot \mathbf{e}_r \, d\Omega, \tag{31}$$

where $\mathbf{e}_m$ is a unit vector perpendicular to $\mathbf{e}_i$. For $\boldsymbol{\alpha}_c = \mathbf{0}$, Eq. (30) therefore equals the magnitude of the total radiation force $\mathbf{F}$ exerted by progressive waves.

https://doi.org/10.1121/10.0043002

The far field of the scattered pressure given by Eq. (9) combined with Φ given by Eq. (25) is to leading order proportional to $(ka)^2$, a result that is consistent with Rayleigh scattering.[68,69] If Eqs. (14) and (15) were instead approximated to zeroth order as $e^{i\mathbf{k}_i\cdot\mathbf{r}_s} \simeq e^{i\mathbf{k}_s\cdot\mathbf{r}_s} \simeq 1$, then the quantity $i(\mathbf{k}_i - \mathbf{k}_s)\cdot\mathbf{r}_s$ would not appear in Φ given by Eq. (16), which when combined with Eq. (9) would reduce to Morse and Ingard's Eq. (8.1.21)[40] and Ginsberg's Eq. (12.3.1):[46]

$$\tilde{p}_s(\mathbf{r}) = p_0 k^2 \frac{e^{ikr}}{4\pi r}(\alpha_m + \alpha_d \mathbf{e}_i\cdot\mathbf{e}_r). \tag{32}$$

The electromagnetic analog of Eq. (32) was originally obtained by Rayleigh to explain why the sky is blue.[70] Since Eq. (32) is based on the assumption that "the phase of any long-wavelength signal will be essentially constant over the extent of the body,"[46] it does not account for the effect of a scatterer's material asymmetry.

The present work generalizes Rayleigh scattering by approximating the phase over the body to linear order. Previous generalizations of Rayleigh scattering include leading-order corrections by Marston[71] to study scattering from and radiation forces on spheres in progressive wave fields. Marston also developed expansions in powers of *ka* to describe acoustic radiation forces exerted by standing waves on spheres.[72,73] Background concerning these expansions is provided in Refs. 74 and 75. Expansions in powers of *ka* were also considered by Stevenson for electromagnetic scattering problems.[76]

The fact that $\underline{\boldsymbol{\alpha}}_d$ given by Eq. (27) is proportional to the identity tensor reflects the fact that "the dipole is aligned in the direction of the incident wave"[46] in the Born approximation. The same result was reported by Marston for scattering of evanescent incident waves from an infinite fluid cylinder.[77] Had the Born approximation not been made, the second term of the integrand of Eq. (6) would be proportional to $\mathbf{k}_s\cdot\nabla_s[\tilde{p}_i(\mathbf{r}_s) + \tilde{p}_s(\mathbf{r}_s)]$ in the far field, revealing for plane wave incidence ($\tilde{p}_i = p_0 e^{i\mathbf{k}_i\cdot\mathbf{r}}$) that $\underline{\boldsymbol{\alpha}}_d \neq \alpha_d\underline{\mathbf{I}}$ only when the gradient of the scattered pressure is oriented in a direction other than $\mathbf{k}_i$. Because $\tilde{p}_s$ is neglected altogether in the Born approximation, the quantity $\mathbf{k}_s\cdot\nabla_s\tilde{p}_i(\mathbf{r}_s)$ is proportional to $\mathbf{e}_r\cdot\mathbf{e}_i$, comparison of which to the last term of Φ given by Eq. (25) shows that $\underline{\boldsymbol{\alpha}}_d$ is proportional to the identity tensor. References 78, 65, 79, 38 and 46 provide methods of obtaining matrix representations of $\underline{\boldsymbol{\alpha}}_d \neq \alpha_d\underline{\mathbf{I}}$ when the scatterer does not satisfy the Born approximation. Cases in which $\underline{\boldsymbol{\alpha}}_d \neq \alpha_d\underline{\mathbf{I}}$ are also encountered in anisotropic subwavelength structures,[57,80,81] although resonance effects preclude such structures from being studied in the Born approximation.[82]

The coupled polarizability given by Eq. (28) differs in several ways from α_m and $\underline{\boldsymbol{\alpha}}_d$ given by Eqs. (26) and (27), respectively. For one thing, $\boldsymbol{\alpha}_c$ is proportional to the wavenumber $k = \omega/c_0$, suggesting that it arises because of a dynamic effect.[55,83,84] The factor of k in $\boldsymbol{\alpha}_c$ combined with the factor of $-i$ in Eqs. (18) and (19) forms the product $-ik = -i\omega/c_0$, which is suggestive of the time derivative of a harmonic quantity. Equations (18) and (19) therefore suggest that the coupled polarizability relates pressure to acceleration $\partial\mathbf{u}/\partial t$, not velocity itself, an interpretation that is consistent with the time-domain form of the macroscopic Willis constitutive relations expressed by Sieck *et al.*[55] When combined with the far field of the scattered pressure given by Eqs. (9) and (25), the coupled polarizability therefore contributes to the scattered field at $O[(ka)^3]$ rather than at $O[(ka)^2]$, as in the case for scattering associated with α_m and $\underline{\boldsymbol{\alpha}}_d$. Because the polarizabilities appear in $|\Phi|^2$ in quadratic combinations, it is anticipated that α_m^2 and α_d^2 contribute to Westervelt's integral at $O[(ka)^4]$, whereas $|\boldsymbol{\alpha}_c|^2$ contributes at $O[(ka)^6]$, as will be shown in Sec. IV.

Another difference between $\boldsymbol{\alpha}_c$ and the monopole and dipole polarizabilities is that the volume integrals in Eq. (28) for $\boldsymbol{\alpha}_c$ are taken not over the contrast factors but over their moments, $\gamma_\beta(\mathbf{r}_s)\mathbf{r}_s$ and $\gamma_\rho(\mathbf{r}_s)\mathbf{r}_s$, indicating that $\boldsymbol{\alpha}_c$ vanishes if $\gamma_\beta(\mathbf{r}_s) = \gamma_\beta(-\mathbf{r}_s)$ and $\gamma_\rho(\mathbf{r}_s) = \gamma_\rho(-\mathbf{r}_s)$ over a symmetric domain. The form of Eq. (28) indicates that $\boldsymbol{\alpha}_c$ is nonzero when the contrast factors are not even functions of $\mathbf{r}_s$.

Finally, it is noted that although Eqs. (26)–(28) are independent of coordinate systems, Eq. (28) does depend on the choice of the origin. The origin $\mathbf{0}$ is defined by Eq. (8) to be the centroid of the scatterer because it is desired that $\boldsymbol{\alpha}_c$ be "nonzero when the inhomogeneity has some form of asymmetry."[55] The use of the centroid as the origin is consistent with previous studies of radiation force[27] and Willis coupling.[55] The relationship between the choice of the origin and the uniqueness of dynamic homogenization schemes is discussed in Refs. 85 and 86.

Expressions of acoustic polarizabilities that depend explicitly on material properties are generally unavailable without relying on approximations like those leading to Eqs. (26)–(28). Previous polarizability formulations are based on inverse scattering, in which the polarizabilities are expressed in terms of scattered fields.[55–57,80] Although such formulations can account for resonant phenomena and strong scattering, their generality comes at the expense of simplicity and physical insight. An appreciation of the complexity of previous studies of acoustic polarizability can be gained by inspecting Eq. (16) of Ref. 56, which itself is based on a formulation that is "significantly simpler than that of [Ref. 57]."[56] In contrast, the present work provides expressions for the scattered field in terms of acoustic polarizabilities, which are calculated by integrating the material properties over the volume of the scatterer. The simplicity of the present formulation is due to the far-field and Born approximations, which limit the generality of the present work.

Sepehrirahnama *et al.*[59–61] employed the inverse scattering formulation of the acoustic polarizabilities derived by Quan *et al.*[57] to calculate the radiation force exerted by both standing and progressive waves on subwavelength scatterers. The present work provides a solution of the corresponding forward problem for the radiation force exerted by progressive waves, although the results presented here differ from those reported by Sepehrirahnama *et al.* The discrepancy appears to result from the claim that "the primary

radiation force acting on a scatterer corresponds to the incident-scattering portion of the time-averaged radiation stresses,"[59] an assumption that is often made in the calculation of radiation force exerted by standing waves.[2,18] Forces due to progressive waves, however, are given in terms of the intensity of the scattered wave,[42,43] as noted by Gor'kov:[2]

> The magnitude of the average force in a standing wave is larger than in a plane running wave. In the former case, in the quadratic expression for the force there are also important contributions from the interference terms between the incident and scattered waves, whereas for a running wave the magnitude of the momentum imparted to the particle by the waves is determined only by the momentum carried away by the scattered wave.

A comparison of the present formulation with that of Sepehrirahnama *et al*. may be discussed in future work.

IV. EXAMPLES

Westervelt's integral given by Eq. (1) is now evaluated in terms of Eqs. (25)–(28) for homogeneous and inhomogeneous spheres and cubes. Although Morse and Ingard's contrast factors given by Eqs. (4) are convenient for the analysis in Secs. II and III, studies of acoustic radiation force more frequently describe the material properties of scatterers in terms of Gor'kov's contrast factors[2,27]

$$f_\beta(\mathbf{r}) = 1 - \frac{\beta_s(\mathbf{r})}{\beta_0}, \quad f_\rho(\mathbf{r}) = \frac{2[\rho_s(\mathbf{r}) - \rho_0]}{2\rho_s(\mathbf{r}) + \rho_0}, \tag{33}$$

which are related to Eq. (4) through

$$f_\beta = -\gamma_\beta, \quad f_\rho = \frac{2\gamma_\rho}{3 - \gamma_\rho}, \tag{34}$$

and therefore $\gamma_\beta = -f_\beta$ and $\gamma_\rho = 3f_\rho/(2 + f_\rho)$. Gor'kov's contrast factors are used below for ease of comparison with previous studies.[2,23,40,87]

The radiation force is normalized by

$$F_0 = \frac{p_0^2 A_\parallel}{2\rho_0 c_0^2}, \tag{35}$$

where $A_\parallel$ is the cross-sectional area of the scatterer encountered by the incident wave. The incident wave is chosen to be oriented in the z direction, so $F_\parallel = F_z$, and the dot product $\mathbf{e}_i \cdot \mathbf{e}_r$ appearing in Eqs. (1), (25), and (28) equals $\mathbf{e}_z \cdot \mathbf{e}_r = \cos\theta$, where θ is the spherical polar angle.

A. Homogeneous sphere

Considered first is the radiation force on a homogeneous compressible sphere of radius a whose material properties are given by $f_\beta = f_1$ and $f_\rho = f_2$, as defined by Eq. (33). According to Eqs. (26)–(28), the polarizabilities are

$$\alpha_m = -\frac{4}{3}\pi a^3 f_1, \quad \alpha_d = \frac{4}{3}\pi a^3 \frac{3f_2/2}{1 + f_2/2}, \tag{36}$$

and $\boldsymbol{\alpha}_c = \mathbf{0}$, where the coupled polarizability is calculated in spherical coordinates (r, θ, ϕ) by noting that $\mathbf{r}_s$ in Eq. (28) equals $r_s(\mathbf{e}_x \sin\theta_s \cos\phi_s + \mathbf{e}_y \sin\theta_s \sin\phi_s + \mathbf{e}_z \cos\theta_s)$.[63] Inserting Eqs. (36) into $F_\parallel$ given by Eq. (30) yields the radiation force in the z direction,

$$\frac{F_z}{F_0} = \frac{4}{9}(ka)^4 \left[f_1^2 + \frac{f_1 f_2}{1 + f_2/2} + \frac{3f_2^2}{4(1 + f_2^2/2)^2} \right], \tag{37}$$

where it has been noted that $A_\parallel = \pi a^2$.

The radiation force on a small sphere due to progressive waves was previously obtained by Gor'kov.[2] Gor'kov's result is recovered from Eq. (37) by noting that the Born approximation underlying Eq. (37) is satisfied if f_1 and f_2 are much less than unity,[23] warranting the binomial expansion of the denominators of the terms in square brackets of Eq. (37):

$$\frac{f_1 f_2}{1 + f_2/2} \simeq f_1 f_2 (1 - f_2/2),$$

$$\frac{3f_2^2}{4(1 + f_2^2/2)^2} \simeq \frac{3}{4} f_2^2 (1 - f_2^2).$$

The Born approximation therefore justifies retaining only the quadratic order of the contrast factors in Eq. (37), yielding

$$F_z = \frac{4\pi \langle I \rangle}{9c_0} a^2 (ka)^4 \left(f_1^2 + f_1 f_2 + \frac{3}{4} f_2^2 \right), \tag{38}$$

where $\langle I \rangle = p_0^2/2\rho_0 c_0 = \rho_0 c_0 u_0^2/2$ is the time-averaged intensity of the incident wave.[67] Equation (38) recovers Gor'kov's Eq. (10).[2]

The validity of Eqs. (37) and (38) is assessed by comparison to the full expression for the radiation force on a homogeneous compressible sphere in terms of spherical wave expansions provided by Refs. 23, 52, and 88. The incident and scattered waves are expressed in terms of the eigenfunctions of the axisymmetric Helmholtz equation in spherical coordinates,

$$\tilde{p}_i = \sum_{n=0}^{\infty} a_n j_n(kr) P_n(\cos\theta), \tag{39}$$

$$\tilde{p}_s = \sum_{n=0}^{\infty} A_n a_n h_n^{(1)}(kr) P_n(\cos\theta), \tag{40}$$

where j_n are the spherical Bessel functions, $h_n^{(1)}$ are the spherical Hankel functions of the first kind, and P_n are the Legendre polynomials. The coefficient $a_n = i^n(2n + 1)$ corresponds to the incident plane wave,[89] whereas A_n corresponds to the scattered wave and is determined by satisfying the continuity of pressure and normal fluid velocity at

https://doi.org/10.1121/10.0043002

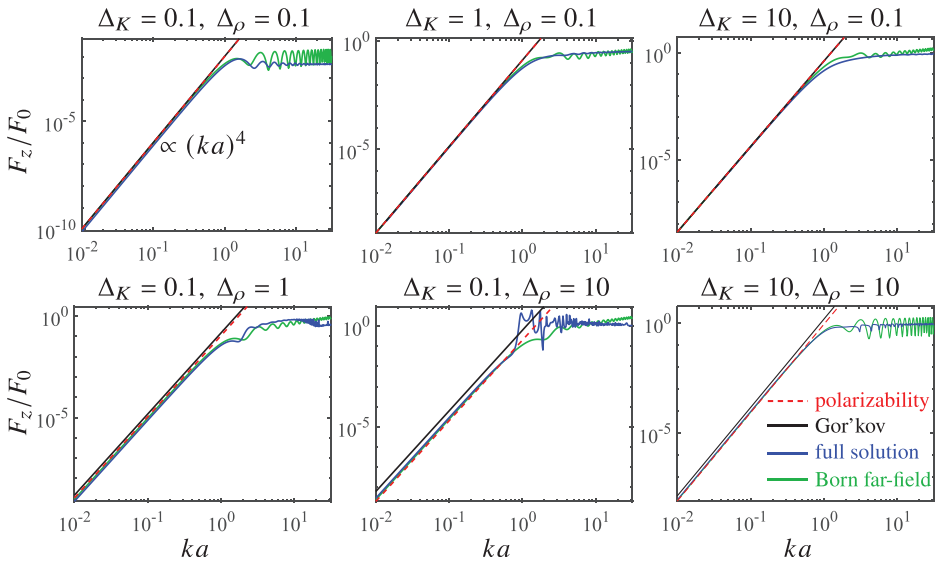

FIG. 5. Comparison of the polarizability-based formulation given by Eq. (37) (dashed red lines), Gor'kov's result for the radiation force on a sphere given by Eq. (38) (solid black lines), the full expression for the radiation force on a sphere given by Eq. (41) (solid blue curves), and the radiation force on a cube having the same volume and material properties as the sphere given by Eq. (51) (solid green curves) as a function of ka. The contrasts $\Delta_K = (K_s - K_0)/K_0$ and $\Delta_\rho = (\rho_s - \rho_0)/\rho_0$ range two orders of magnitude, where the top-left plot corresponds to a scatterer with weak material contrast and the bottom-right plot approximates a rigid scatterer.

$r = a$.[90] The radiation force is given by Eq. (3) of Jerome *et al.*,[23] the normalized form of which is

$$\frac{F_z}{F_0} = \mathrm{Re}\left[\frac{4i}{(ka)^2}\sum_{n=0}^{\infty}\frac{n+1}{(2n+1)(2n+3)} \times (A_n^* + A_{n+1} + 2A_n^* A_{n+1})a_n^* a_{n+1}\right]. \tag{41}$$

Equations (37), (38), and (41) are compared for six combinations of contrast factors in Fig. 5. The numerical evaluation of the summation in Eq. (41) is truncated to the first 70 terms, which is sufficient for convergence of the summation to $ka \simeq 90$. To aid the characterization of the material properties, the dimensionless quantities

$$\Delta_K = (K_s - K_0)/K_0, \qquad \Delta_\rho = (\rho_s - \rho_0)/\rho_0 \tag{42}$$

introduced by Jerome *et al.*[23] are used, where $K_s = 1/\beta_s$ and $K_0 = 1/\beta_0$ are the bulk moduli of the sphere and the background medium, respectively. Equation (42) is related to f_1 and f_2 by

$$f_1 = \frac{\Delta_K}{1+\Delta_K}, \qquad f_2 = \frac{\Delta_\rho}{1+\frac{2}{3}\Delta_\rho}, \tag{43}$$

which show that the low-contrast condition $|f_1|, |f_2| \ll 1$ is equivalent to $|\Delta_K|, |\Delta_\rho| \ll 1$, for which Eq. (43) becomes $f_1 \simeq \Delta_K$ and $f_2 \simeq \Delta_\rho$.

The solid black lines in Fig. 5 show that neglecting terms of cubic order and higher in the contrast factors leads to error for cases in which the contrast in density is much greater than the contrast in bulk modulus ($\Delta_\rho/\Delta_K \gg 1$). In such cases, Gor'kov's result given by Eq. (38) over-predicts the radiation force. The polarizability-based formulation given by Eq. (37), represented by the dashed red curves, recovers the subwavelength limit of the full solution given by Eq. (41) for all combinations of Δ_K and Δ_ρ considered.

The accuracy of the polarizability-based formulation for cases in which the material contrast is large reflects the fact that the Born approximation holds if the scatterer is sufficiently smaller than a wavelength. The same observation was made by Jerome *et al.* regarding the Born approximation of radiation forces exerted by standing waves,[23] as mentioned in Secs. I and II. In the present work, the Born approximation holds for sufficiently low values of ka because in the absence of resonance, the smallness of the scatterer with respect to a wavelength guarantees that the magnitude of the scattered field is much weaker than that of the incident field, allowing $\tilde{p}_s$ to be neglected in Eq. (6). The Born approximation of Jerome *et al.*[23] is satisfied for low ka because the volume of integration converges to a point as ka tends to zero, and the integral for the radiation force converges to the value of the integrand at that point. Because the integrand given by Eq. (7) of Jerome *et al.*[23] is derived from the small particle limit of the full solution given by Eq. (41), the Born approximation of the radiation force exerted by standing waves converges to the full expression for $ka \ll 1$ regardless of material contrast. More insight into scattering from small totally reflective spheres is provided on pp. 158–161 of Ref. 39.

Although the focus of the present work is the study of radiation force in the subwavelength regime, an explanation is owed to why the high-frequency asymptote of the radiation force on a rigid sphere is $F_z = F_0$, as suggested by the solid blue curve in the bottom-right plot in Fig. 5. The high-frequency asymptote of the force can be calculated by considering the limit $ka \gg 1$ of the time-averaged scattered intensity from a rigid sphere, given by the second of Morse and Ingard's Eq. (8.2.3).[40] From Eq. (A13), the corresponding magnitude squared of the scattered directivity is

$$|\Phi|^2 = \frac{1}{4}a^2\left[1 + \cot^2(\theta/2)J_1^2(ka\sin\theta)\right], \qquad ka \gg 1, \tag{44}$$

where J_1 is the cylindrical Bessel function of order 1. Inserting Eq. (44) into Westervelt's integral yields

$$F_z = \frac{p_0^2}{2\rho_0 c_0^2}(2\pi a^2 - \pi a^2) = F_0, \qquad ka \gg 1, \tag{45}$$

where $\oint |\Phi|^2 d\Omega$ is given by the last of Morse and Ingard's Eqs. (8.2.3),[40] and $-\oint |\Phi|^2 \mathbf{e}_i \cdot \mathbf{e}_r \, d\Omega$ is calculated numerically. Equation (45) was obtained previously by Marston,[91] and form functions for $ka = 15$ are shown in Fig. 2 of Ref. 92. An alternative calculation of the same result from the perspective of ray theory was obtained by Marston *et al.*[93,94]

B. Homogeneous cube

Considered next is the radiation force on a homogeneous cube whose volume and material properties are equal to those of the homogeneous sphere considered above. The side length of the cube is therefore $b = a(4\pi/3)^{1/3}$. The polarizabilities given by Eqs. (26)–(28) are evaluated in Cartesian coordinates, where the domain of integration is

$$|x_s| \le b/2, \qquad |y_s| \le b/2, \qquad |z_s| \le b/2, \tag{46}$$

yielding

$$\alpha_m = -b^3 f_1, \qquad \alpha_d = b^3 \frac{3f_2/2}{1 + f_2/2}, \tag{47}$$

and $\boldsymbol{\alpha}_c = \mathbf{0}$. Inserting Eqs. (47) into $F_\parallel$ given by Eq. (30) and writing the result in terms of a again yields Eq. (37).

Assessing whether Eq. (37) accurately predicts the radiation force on a homogeneous subwavelength cube is challenging because no analytical expressions analogous to Eq. (41) are available for cubes.[95] Although approximations for the field scattered by a homogeneous cube have been derived using the anomalous diffraction approximation,[96,97] such solutions are restricted to $ka \gg 1$. It is possible, however, to calculate the radiation force in the far field of the Born approximation by inserting Φ given by Eq. (10) (which holds for all ka) into Westervelt's integral. Comparing the result with Eq. (37) allows for the validity of the subwavelength approximation underlying Eq. (37) to be assessed, although the comparison does not account for the error associated with large material contrasts and resonances. Scattering from rigid cubes is discussed in a recent publication by Ospel.[98]

Evaluating Eq. (10) over the domain given by Eq. (46) yields

$$\Phi(\mathbf{k}_s) = \frac{1}{3}k^2 a^3 f(\mathbf{k}_s)\left(-f_1 + \frac{3f_2/2}{1 + f_2/2}\cos\theta\right), \tag{48}$$

$$f(\mathbf{k}_s) = \prod_{j=1}^{3} \frac{\sin\left[(k_{sj} - k_{ij})b/2\right]}{(k_{sj} - k_{ij})b/2}, \tag{49}$$

where $j = 1, 2$, and 3, represent x, y, and z, respectively, and where the three-dimensional (3D) Fourier transform in Eq. (10) has been evaluated using the shifting property,[99]

$$\mathcal{F}_{3D}\left\{f(x,y,z)e^{i(\alpha x + \beta y + \gamma z)}\right\} = F(k_{sx} - \alpha, k_{sy} - \beta, k_{sz} - \gamma). \tag{50}$$

Westervelt's integral therefore equals

$$\frac{F_z}{F_0} = \int_0^{2\pi}\int_0^{\pi} |\Phi(\theta,\phi)/a|^2 (1 - \cos\theta)\sin\theta \, d\theta \, d\phi, \tag{51}$$

where Φ is given by Eq. (48). Equation (51) is evaluated numerically and is plotted as the solid green curves in Fig. 5, where it is compared with the polarizability-based force given by Eq. (37) and the full expression of the force on a sphere having the same volume and material properties given by Eq. (41).

The coincidence of the dashed red curves representing Eq. (37) with the solid green curves representing Eq. (51) for $ka \ll 1$ in Fig. 5 demonstrates the validity of the subwavelength approximation leading to the polarizabilities given by Eqs. (25)–(28). The coincidence of the solid green curves with the solid blue curves representing the full expression of the force on a sphere of equal volume and material properties shows that "geometric details that are much smaller than the wavelength are unimportant,"[46] i.e., the edges and corners of the cube that distinguish it from the sphere cannot be resolved for $ka \ll 1$. The coincidence of the green and blue curves in Fig. 5 also shows that the Born approximation leading to Eq. (10) is satisfied if ka is sufficiently small regardless of material contrast, as discussed in Sec. II.

C. Three-layered sphere

Attention is now turned to radiation forces exerted by plane progressive waves on inhomogeneous objects. A three-layered sphere is considered because such objects have previously been used to model radiation forces exerted by standing waves on eukaryotic cells.[27,87,100,101] The inner, middle, and outer radii are denoted by a'', a', and a, respectively, as shown in the inset of Fig. 6.

The contrast factors f_β and f_ρ are given by f_1'' and f_2'' for $r \le a''$, f_1' and f_2' for $a'' < r \le a'$, and f_1 and f_2 for $a' < r \le a$, respectively, where the numerical values of the

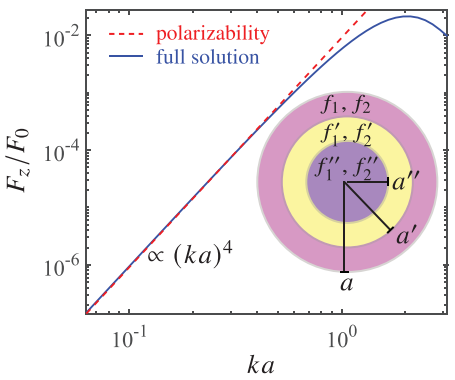

FIG. 6. Comparison of the polarizability-based formulation given by Eq. (30) in terms of Eqs. (52) and (53) (dashed red line) and the full expression based on spherical wave expansions (Ref. 101) (solid blue curve) for the radiation force on a three-layered sphere as a function of ka, where the dimensions and material properties are provided in Table I of Wang *et al.* (Ref. 87).

https://doi.org/10.1121/10.0043002

parameters are provided in Table I of Refs. 87 and 101. Evaluating Eqs. (26)–(28) in this case yields

$$\alpha_{\mathrm{m}} = -\frac{4}{3}\pi a^3\left[f_1''\chi'' + f_1'(\chi' - \chi'') + f_1(1-\chi')\right], \tag{52}$$

$$\alpha_{\mathrm{d}} = \frac{4}{3}\pi a^3\left[\frac{3f_2''/2}{1+f_2''/2}\chi'' + \frac{3f_2'/2}{1+f_2'/2}(\chi' - \chi'') + \frac{3f_2/2}{1+f_2/2}(1-\chi')\right], \tag{53}$$

and $\boldsymbol{\alpha}_{\mathrm{c}} = \mathbf{0}$, where $\chi' = (a'/a)^3$ and $\chi'' = (a''/a)^3$ are the volume fractions of the regions enclosed by the middle and inner radii, respectively. Equations (52) and (53) in combination with Eq. (30) for $F_{\parallel}$ yields the Born approximation of the radiation force, which is compared with the full expression given by Eq. (10) of Ref. 101.

Equation (30) and the full expression are normalized by Eq. (35) for $A_{\parallel} = \pi a^2$ and are compared in Fig. 6. The agreement between the polarizability-based formulation and the full expression for $ka \ll 1$ shows that the present formulation accurately predicts forces exerted by progressive waves on subwavelength scatterers with segmented inhomogeneities that satisfy the Born approximation.

An analysis that includes resonance effects of concentric fluid spheres in standing wave fields was provided recently by Marston.[75]

D. Inhomogeneous cube

Finally, an inhomogeneous cube of side length a whose material properties are given by $f_\beta = -2f_1 x_{\mathrm{s}}/a$ and $f_\rho = 4f_2(x_{\mathrm{s}}/a)/(3 - 2f_2 x_{\mathrm{s}}/a)$ is considered. The material properties are chosen such that Eqs. (26)–(28) yield $\alpha_{\mathrm{m}} = \alpha_{\mathrm{d}} = 0$ but $\boldsymbol{\alpha}_{\mathrm{c}} \neq \mathbf{0}$, as shown below, allowing for the effect of the coupled polarizability on the radiation force to be studied independently of the monopole and dipole polarizabilities. The radiation force in the direction of the incident wave is calculated for two incident-wave orientations: $\mathbf{e}_{\mathrm{i}} = \mathbf{e}_z$ and $\mathbf{e}_{\mathrm{i}} = \mathbf{e}_x$.

1. Incident wave in z direction

The incident wave oriented in the z direction is described by setting $\mathbf{e}_{\mathrm{i}} = \mathbf{e}_z$, for which Eq. (28) in terms of the material properties defined above yields

$$\boldsymbol{\alpha}_{\mathrm{c}} = \frac{1}{6}ka^4(f_1 + f_2\cos\theta)\mathbf{e}_x. \tag{54}$$

Equation (54) is inserted into Φ given by Eq. (25), which is in turn inserted into Eq. (1) for the radiation force in the direction of the incident wave, yielding

$$\frac{F_z}{F_0} = \frac{(ka)^6}{432\pi}\left[f_1^2 + \frac{1}{5}(f_2^2 - 2f_1 f_2)\right]. \tag{55}$$

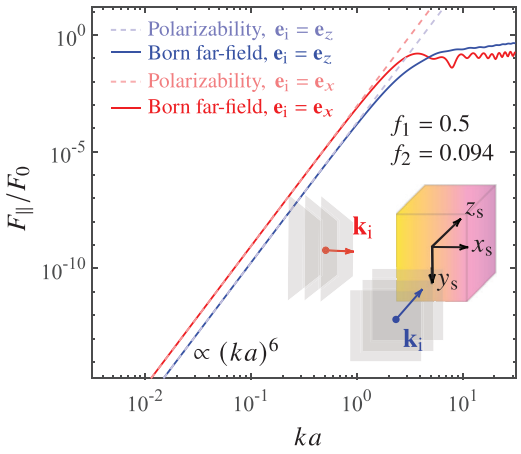

FIG. 7. Radiation force in the direction of the incident wave as a function of ka on an inhomogeneous cube. The blue and red curves denote the force exerted by an incident wave traveling along the z and x directions, respectively. For z incidence, the force given by Eq. (55) (dashed light blue line) is compared with Eq. (51) in terms of Eq. (56) (solid dark blue line). For x incidence, the force given by Eq. (59) (dashed light red line) is compared with Eq. (60) in terms of Eq. (61) (solid dark red line).

As anticipated in Sec. III, $|\boldsymbol{\alpha}_{\mathrm{c}}|^2$ contributes to the radiation force at $O[(ka)^6]$.

Equation (55) is compared in Fig. 7 with the force predicted in the far field of the Born approximation given by Eq. (51), where Φ given by Eq. (10) yields

$$\Phi(\mathbf{k}_{\mathrm{s}}) = \frac{k^2a^3}{4\pi}f(\mathbf{k}_{\mathrm{s}})(f_1 + f_2\cos\theta), \tag{56}$$

$$f(\mathbf{k}_{\mathrm{s}}) = \left\{\cos[(k_{\mathrm{s}x} - k_{\mathrm{i}x})a/2] - \frac{\sin[(k_{\mathrm{s}x} - k_{\mathrm{i}x})a/2]}{(k_{\mathrm{s}x} - k_{\mathrm{i}x})a/2}\right\} \times \frac{i}{(k_{\mathrm{s}x} - k_{\mathrm{i}x})a/2}\prod_{j=2}^{3}\frac{\sin[(k_{\mathrm{s}j} - k_{\mathrm{i}j})a/2]}{(k_{\mathrm{s}j} - k_{\mathrm{i}j})a/2}, \tag{57}$$

where $k_{\mathrm{i}z} = k$ and $k_{\mathrm{i}x} = k_{\mathrm{i}y} = 0$. The contrast factors $f_1 = 0.5$ ($\Delta_K = 1$) and $f_2 = 0.094$ ($\Delta_\rho = 0.1$) are used for the comparison. The agreement for $ka \ll 1$ between the dashed light blue lines representing Eq. (55) and the solid blue curves representing the numerical evaluation of Eq. (51) in terms of Eq. (56) demonstrates that the present formulation accurately predicts the radiation force due to progressive waves on a subwavelength object with a continuous and asymmetric distribution of material inhomogeneity.

The fact that $\boldsymbol{\alpha}_{\mathrm{c}}$ given by Eq. (54) breaks axisymmetry raises the question of whether the incident wave oriented in the z direction exerts a radiation force on the inhomogeneous cube in either of the transverse directions. The force in the x direction to dipole order vanishes, as can be seen by inserting the directivity Φ given by Eq. (25) in terms of Eq. (54) into Westervelt's integral for $F_\perp$ given by Eq. (31) for $\mathbf{e}_m = \mathbf{e}_x$, where it is noted that $\mathbf{e}_x \cdot \mathbf{e}_r = \sin\theta\cos\phi$. Meanwhile, in the far field of the Born approximation, Φ given by Eq. (56) is inserted into Eq. (31), yielding a force

that is proportional to $(ka)^6$ but is five orders of magnitude weaker than Eq. (55) for $ka \ll 1$. Evidently, at the order of the present approximation, radiation forces in transverse directions are due to effects higher than dipole order, which are accounted for in Φ given by Eq. (56) but not in Eq. (25). The force in the y direction, which is calculated by setting $\mathbf{e}_y \cdot \mathbf{e}_r = \sin\theta \sin\phi$, vanishes both in the far field of the Born approximation and in its subwavelength limit.

The prediction by the present formulation of zero transverse radiation forces on asymmetric objects is not surprising given the similar limitation on the Born approximation made by Jerome *et al.* that the transverse components "are simply not predicted by the model for the prescribed standing wave field."[23] The fact that the force in the x direction calculated by Eq. (31) in terms of Eq. (56) is five orders of magnitude weaker than F_z given by Eq. (55) is reminiscent of the finding for standing waves that "when the conditions for the validity of the Born approximation are satisfied, the magnitudes of the transverse forces may be presumed small in relation to that of F_z."[23] The use of "large objects (> 20 wavelengths)" by Zhang and Ma to experimentally generate transverse radiation forces exerted by progressive waves[32] suggests that such forces become sizable for $ka \gg 1$.

2. Incident wave in x direction

The incident wave is now chosen to be oriented in the direction of $\mathbf{e}_x$, whereas the orientation of the cube is left unchanged. The coupled polarizability given by Eq. (28) therefore becomes

$$\boldsymbol{\alpha}_c = \frac{1}{6} ka^4 (f_1 + f_2 \sin\theta \cos\phi)\mathbf{e}_x, \tag{58}$$

and Westervelt's integral yields the force in the direction of the incident wave as

$$\frac{F_x}{F_0} = \frac{(ka)^6}{72\pi}\left(f_1^2 - \frac{6}{5} f_1 f_2 + \frac{7}{15} f_2^2\right). \tag{59}$$

In Fig. 7, Eq. (59) is plotted as the dashed light red line and compared with the solid red curve, which represents the force predicted in the far field of the Born approximation given by

$$\frac{F_x}{F_0} = \int_0^{2\pi}\int_0^{\pi} |\Phi(\theta,\phi)/a|^2 (1 - \sin\theta\cos\phi)\sin\theta \, \mathrm{d}\theta \, \mathrm{d}\phi, \tag{60}$$

where from Eq. (10),

$$\Phi(\mathbf{k}_s) = \frac{k^2 a^3}{4\pi} f(\mathbf{k}_s)(f_1 + f_2 \sin\theta\cos\phi), \tag{61}$$

and where $f(\mathbf{k}_s)$ is given by Eq. (57) with $k_{ix} = k$ and $k_{iy} = k_{iz} = 0$.

Comparison of Eqs. (55) and (59) in Fig. 7 reveals that the force aligned with the gradient of the material properties is greater than that perpendicular to the gradient of the material properties by an amount given by the ratio of Eq. (59) to Eq. (55), which in turn depends not on f_1 and f_2 but on $\Delta = f_1/f_2$:

$$\frac{F_x}{F_z} = 2\frac{\Delta^2 - 6\Delta/5 + 7/15}{\Delta^2/3 + (1 - 2\Delta)/15}. \tag{62}$$

For the material properties considered in Fig. 7, $\Delta = 5.3$ and Eq. (62) equals $F_x/F_z = 5.1$. If the cube differs from the background medium only by its density, $\Delta = 0$ and $F_x/F_z = 14$; if the cube differs from the background medium only by its compressibility, then $\Delta = \infty$ and $F_x/F_z = 6$.

Equation (62) raises the question of how the ratio depends on the material distribution. For example, consider an inhomogeneous cube of side length a consisting of two halves with material properties $f_\beta = f_1$ and $f_\rho = -2f_2/(3 + f_2)$ for $-a/2 \le x < 0$, and $f_\beta = -f_1$ and $f_\rho = 2f_2/(3 - f_2)$ for $0 \le x \le a/2$. Following the analysis above shows that F_z/F_0 and F_x/F_0 in this case are 9/4 times Eqs. (55) and (59), respectively. The values of F_z/F_0 and F_x/F_0 are in agreement with the numerical evaluation of Eqs. (51) and (60) for Φ given by Eqs. (56) and (61), respectively, where

$$f(\mathbf{k}_s) = \{1 - \cos[(k_{sx} - k_{ix})a/2]\} \times \frac{i}{(k_{sx} - k_{ix})a/2} \prod_{j=2}^{3} \frac{\sin[(k_{sj} - k_{ij})a/2]}{(k_{sj} - k_{ij})a/2}. \tag{63}$$

Thus F_x/F_z again results in Eq. (62) in the subwavelength limit, showing that such ratios are generally not unique to a given material distribution of a scatterer. A more complete exploration of how F_x/F_z depends on different material distributions may be pursued in the future.

V. CONCLUSION AND APPLICATIONS

Radiation forces exerted by plane progressive acoustic waves on subwavelength scatterers were calculated in terms of acoustic polarizabilities. The Born approximation allowed the monopole and dipole polarizabilities to be expressed as volume integrals over the material contrast factors. For homogeneous objects, the force is on the order of $(ka)^4$, as predicted by Gor'kov for a homogeneous sphere. It was found by comparison with the full expression of radiation force in terms of spherical wave expansions that Gor'kov's result is inaccurate for cases in which the contrast in density is much larger than the contrast in compressibility, whereas the present formulation is accurate for all material contrasts considered. For $ka \ll 1$, an identical radiation force is exerted on a homogeneous cube with the same material properties and volume as a homogeneous sphere. Inhomogeneous scatterers with compressibility and density contrast factors that are even functions of position also experience a radiation force on the order of $(ka)^4$.

Material asymmetry was taken into account by extending Rayleigh scattering to $O[(ka)^3]$, leading to a volume

integral for the coupled polarizability over the moment of the contrast factors. The coupled polarizability, which depends on both the frequency and direction of the incident wave, vanishes in the static limit and/or in the absence of material asymmetry, in which case the present formulation recovers Rayleigh scattering. Scatterers with odd compressibility and density contrast factors experience a radiation force on the order of $(ka)^6$. By considering an inhomogeneous cube with an asymmetric distribution of material properties, it was shown that material asymmetry leads to anisotropic radiation forces, i.e., forces that depend on the direction of the incident wave. The preferential direction in which the inhomogeneous cube is forced may find application in particle manipulation for advanced manufacturing.[102]

The error associated with the far-field, Born, and subwavelength approximations leading to the integral expressions for the acoustic polarizabilities was also discussed. Although the far-field approximation is consistent with Westervelt's integral and introduces no error in the calculation of radiation force, the Born and subwavelength approximations introduce error when material contrasts are large and when the scatterer is larger than $ka \sim 0.8$. It was demonstrated by comparison with full expression of forces that the Born approximation can be satisfied for $ka \ll 1$ even when material contrasts are large. The interdependence of the Born and subwavelength approximations was discussed in the context of previous works.

The expressions derived may model the radiation force exerted by paraxial beams to reasonable accuracy because the incident waves of high-frequency beams are quasiplanar. For example, the force on a subwavelength dielectric sphere suspended in an optical beam[103] has a functional form similar to the polarizability-based force given by Eq. (37), suggesting that the force in the direction of the primary direction of incident wave motion can be approximated locally by the results of the present work. Transverse forces exerted by beams act as standing wave fields conducive to the Born approximation developed by Jerome *et al.*,[23] as discussed by Fan and Zhang.[104]

Acoustofluidic devices like those described by Jo and Guldiken[105] similarly involve a combination of standing and progressive wave fields. The force exerted by the standing wave component on biological media is conducive to the Born approximation developed by Jerome *et al.*, as shown in Ref. 101, whereas the present work provides a means to calculate the radiation force exerted by the progressive wave component.

A subwavelength Born scatterer characterized by nonzero values of α_m, α_d, and $\boldsymbol{\alpha}_c$ experiences radiation forces of orders $(ka)^4$ [associated with the first three terms of Eq. (29)] and $(ka)^6$ [associated with the last term of Eq. (29)]. Such scatterers were not considered as examples in the present work, but their application to the design of particles that experience desired forces[58] may be explored in the future.

Another avenue of future work is the consideration of acoustic radiation torque, which can be calculated using the far-field directivity in the Born approximation given by Eq. (10) or its subwavelength limit given by Eq. (25) in combination with Maidanik's formulation for the torque exerted by plane progressive waves.[106] The inhomogeneous cube considered in Sec. IV experiences zero radiation torque at dipole order for both configurations of the incident wave, but the inclusion of higher-order terms in the multipole expansion may lead to interesting dynamics related to the angular stability of the scatterer.

Although the present work provides the low-*ka* asymptote of radiation force exerted by plane progressive waves in the Born approximation, the high-*ka* asymptote of radiation force exerted on inhomogeneous and/or asymmetric objects may be pursued in the future. Figures 5–7 show that as *ka* becomes large, the radiation force converges to a constant as the effects of diffraction are suppressed. High-*ka* asymptotes of radiation force[107] on canonical objects like spheres[93] [see Eq. (45)] and cylinders[94] may be used to benchmark ray-based approximations developed in the future.

ACKNOWLEDGMENTS

C.A.G. was supported by the Applied Research Laboratories Chester M. McKinney Graduate Fellowship in Acoustics.

AUTHOR DECLARATIONS

Conflict of Interest

The authors have no conflicts to disclose.

DATA AVAILABILITY

The data that support the findings of this study are available from the corresponding author upon reasonable request.

APPENDIX A: WESTERVELT'S FAR-FIELD INTEGRAL

The present work utilizes Westervelt's integral for radiation force in the direction of an incident progressive wave,[42] a result that Westervelt himself felt the need to clarify.[43] The steps leading to Eq. (2) of Ref. 43 are briefly reviewed, and the final step of Westervelt's derivation is elucidated by invoking energy conservation.

Momentum conservation at quadratic order requires that a scatterer of characteristic size a insonified by an arbitrary time-harmonic acoustic wave in an unbounded medium of mass density ρ_0 experiences a force equal to[43]

$$\mathbf{F} = \oint_A \langle \underline{\mathbf{I}} L - \rho_0 \mathbf{u} \otimes \mathbf{u} \rangle \cdot \mathrm{d}\mathbf{A}, \tag{A1}$$

where $\langle \cdots \rangle$ denotes the time average over the period and $\underline{\mathbf{I}}$ is the identity tensor. The differential area $\mathrm{d}\mathbf{A}$ equals $\mathbf{e}_r \, \mathrm{d}A$, where $\mathbf{e}_r$ is the unit outward normal vector of a spherical surface A whose radius is much larger than $ka^2/2$. The quantity L equals the Lagrangian density $T - U$, where $T = \rho_0 u^2/2$ and $U = p^2/2\rho_0 c_0^2$ are the kinetic and potential energy densities,

respectively. The acoustic pressure p and fluid velocity $\mathbf{u}$ correspond to the sum of incident and scattered waves

$$p = p_\mathrm{i} + p_\mathrm{s}, \qquad \mathbf{u} = \mathbf{u}_\mathrm{i} + \mathbf{u}_\mathrm{s}, \tag{A2}$$

where $u^2 = \mathbf{u} \cdot \mathbf{u}$. Westervelt's limiting procedure leading to Eq. (A1) is "not straightforward,"[108] and "it is very difficult…to gain a correct understanding of his theory as it is."[109] An accessible derivation of the indicial form of Eq. (A1) is provided by Wang and Lee.[110] Although dissipation is neglected in the present work, a more general version of Eq. (A1) that accounts for dissipative effects is provided by Doinikov.[111]

In Refs. 42 and 43, Westervelt simplifies Eq. (A1) for incident plane progressive waves, in which case p_i and $\mathbf{u}_\mathrm{i}$ in Eq. (A2) are related through the plane wave impedance relation $p_\mathrm{i}\mathbf{e}_\mathrm{i} = \mathbf{u}_\mathrm{i}\rho_0 c_0$, where $\mathbf{e}_\mathrm{i} = \mathbf{k}_\mathrm{i}/k$ is the unit vector pointing in the direction of the incident wave vector $\mathbf{k}_\mathrm{i}$. Because the kinetic and potential energy densities of plane progressive waves are equal,[38] and because $\mathbf{u}_\mathrm{s} = p_\mathrm{s}\mathbf{e}_r/\rho_0 c_0$ may be used in the far field of the scattered wave,[67] Eq. (A1) simplifies to

$$\mathbf{F} = -\frac{1}{c_0}\oint_A \langle p_\mathrm{i} u_\mathrm{s}\mathbf{e}_\mathrm{i} + p_\mathrm{s} u_\mathrm{i}\mathbf{e}_r + p_\mathrm{s}\mathbf{u}_\mathrm{s}\rangle \, \mathrm{d}A. \tag{A3}$$

The component of the force in the direction of the incident wave is obtained by taking the inner product of both sides of Eq. (A3) with $\mathbf{e}_\mathrm{i}$, moving $\mathbf{e}_\mathrm{i}$ inside the surface integral, and denoting $\mathbf{e}_r \cdot \mathbf{e}_\mathrm{i} = \cos\psi$ (see Fig. 1):

$$F_\parallel = -\frac{1}{c_0}\oint_A \langle p_\mathrm{i} u_\mathrm{s} + (p_\mathrm{s} u_\mathrm{i} + p_\mathrm{s} u_\mathrm{s})\cos\psi\rangle \mathrm{d}A. \tag{A4}$$

Although unit vectors cannot in general be moved inside integrals,[63] the operation leading to Eq. (A4) is justified because the incident wave is assumed to be planar. Thus $\mathbf{e}_\mathrm{i}$ can always be represented by a linear combination of Cartesian unit vectors, which, unlike curvilinear unit vectors, do not depend on position $\mathbf{r}$.

Equation (A4) recovers Eq. (13) of Ref. 43, from which Westervelt obtains Eq. (2) of Ref. 43 by resorting to Lamb's argument that the surface integral in the far field over $\langle p_\mathrm{i}\mathbf{u}_\mathrm{s} + p_\mathrm{s}\mathbf{u}_\mathrm{i}\rangle$ equals "the total rate at which energy is withdrawn from the [incident] waves, in consequence of the presence of the obstacle."[112] The connection between Lamb's statement and Eq. (14) of Ref. 43 is not immediately clear, motivating the following discussion in which Eq. (2) of Ref. 43 is obtained from Eq. (A4) by appealing to energy conservation.

In the absence of acoustic sources and sinks, energy conservation requires that[38]

$$\nabla \cdot \mathbf{I} + \frac{\partial E}{\partial t} = 0, \tag{A5}$$

where $\mathbf{I} = p\mathbf{u}$ is the instantaneous intensity and $E = T + U$ is the total instantaneous acoustic energy density. Integrating Eq. (A5) over the volume enclosed by A, invoking the divergence theorem, and taking the time average yields

$$\oint_A \langle \mathbf{I}\rangle \cdot \mathrm{d}\mathbf{A} = 0, \tag{A6}$$

which has exploited the fact that the time average of the time derivative of a product of two time-harmonic functions vanishes.[110] Equation (A6) states that the energy flux through surface A is zero in the absence of sources and sinks in the volume enclosed by A. Two scenarios of Eq. (A6) are now considered. The first scenario, shown in Fig. 8(a), features an incident plane progressive wave that originates from outside the surface A propagating in the absence of the scatterer. In such a case, no scattered waves are generated, and Eq. (A6) combined with Eq. (A2) yields

$$\oint_A \langle p_\mathrm{i}\mathbf{u}_\mathrm{i}\rangle \cdot \mathrm{d}\mathbf{A} = 0. \tag{A7}$$

In the second scenario, a scatterer is introduced, as shown in Fig. 8(b), resulting in scattered waves. In this case, Eq. (A6) combined with Eqs. (A2) yields

$$\oint_A \langle p_\mathrm{i}\mathbf{u}_\mathrm{i} + p_\mathrm{s}\mathbf{u}_\mathrm{s} + p_\mathrm{s}\mathbf{u}_\mathrm{i} + p_\mathrm{i}\mathbf{u}_\mathrm{s}\rangle \cdot \mathrm{d}\mathbf{A} = 0. \tag{A8}$$

Equations (A7) and (A8) are equal because the scatterer is passive; introduction of the scatterer therefore does not contribute to the energy flux through A. Combining Eqs. (A7) and (A8) and recalling that $\mathrm{d}\mathbf{A} = \mathbf{e}_r \, \mathrm{d}A$, $\mathbf{u}_\mathrm{s} = u_\mathrm{s}\mathbf{e}_r$, and $\mathbf{u}_\mathrm{i} = u_\mathrm{i}\mathbf{e}_\mathrm{i}$ yields

$$\oint_A \langle p_\mathrm{i} u_\mathrm{s} + p_\mathrm{s} u_\mathrm{i}\cos\psi + p_\mathrm{s} u_\mathrm{s}\rangle \, \mathrm{d}A = 0. \tag{A9}$$

Subtracting $\oint_A \langle p_\mathrm{s} u_\mathrm{s}\rangle(1 - \cos\psi)\mathrm{d}A$ from both sides of Eq. (A9) and dividing by $-c_0$ yields

$$\frac{1}{c_0}\oint_A \langle p_\mathrm{s} u_\mathrm{s}\rangle(1 - \cos\psi)\,\mathrm{d}A = -\frac{1}{c_0}\oint_A \langle p_\mathrm{i} u_\mathrm{s} + (p_\mathrm{s} u_\mathrm{i} + p_\mathrm{s} u_\mathrm{s})\cos\psi\rangle \, \mathrm{d}A. \tag{A10}$$

Comparing Eqs. (A4) and (A10) yields

$$F_\parallel = \frac{1}{c_0}\oint_A \langle p_\mathrm{s} u_\mathrm{s}\rangle(1 - \cos\psi)\,\mathrm{d}A, \tag{A11}$$

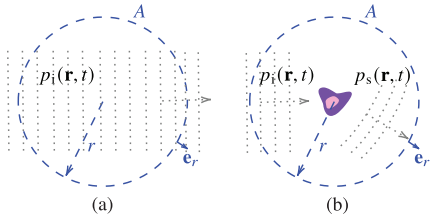

FIG. 8. (a) In the absence of a scatterer, the incident plane progressive wave p_i, which originates from outside the region enclosed by surface A, propagates unperturbed through A. The energy flux through A is given by Eq. (A7). (b) In the presence of a scatterer, some of the incident wave is perturbed, generating the scattered wave p_s. The energy flux through A is given by Eq. (A9).

https://doi.org/10.1121/10.0043002

which recovers Eq. (2) of Ref. 43 for a lossless scatterer. Equation (A11) also recovers Gor'kov's Eq. $(8')$[2] upon noting that $p_s u_s/c_0 = \rho_0 u_s^2$ in the far field.

In terms of the complex-valued functions used to represent time-harmonic wave fields in Sec. II, the pressure and fluid velocity of the scattered wave can be represented in the far field by Eq. (9) and

$$\tilde{u}_s = \frac{p_0}{\rho_0 c_0}\frac{e^{ikr}}{r}\Phi(\mathbf{k}_s), \tag{A12}$$

respectively, where the physical pressure and fluid velocity fields are given by Eq. (3) and $u(\mathbf{r},t) = \mathrm{Re}[\tilde{u}(\mathbf{r})e^{-i\omega t}]$, respectively. The time average of the scattered intensity appearing in Eq. (A11) therefore equals[67]

$$\langle p_s u_s \rangle = \frac{p_0^2}{2\rho_0 c_0}\frac{|\Phi(\mathbf{k}_s)|^2}{r^2}, \tag{A13}$$

insertion of which into Eq. (A11) yields Eq. (1), where $\mathrm{d}\Omega = r^{-2}\,\mathrm{d}A$ is the differential solid angle.

Marston provides additional perspectives on Westervelt's integral in Ref. 91, in which the axisymmetric form of Eq. (1) is obtained. A generalized form of Westervelt's result appropriate for Bessel beams is provided by Zhang and Marston.[44,113] For discussions of Westervelt's integral in the context of the optical theorem, see Refs. 91, 108, 113, and 114. More insight into the physical meaning of the cross-terms $\langle p_i \mathbf{u}_s + p_s \mathbf{u}_i \rangle$ is provided by Marston and Zhang.[115]

APPENDIX B: SCATTERING FROM HETEROGENEITIES

The following derivation of Eqs. (2) and (6) combines the approaches taken by Morse and Ingard[40] and Pierce.[38] Although Morse and Ingard allow the spatial heterogeneities to be arbitrary functions of time, Pierce does not; the latter assumption is made here.

Begin by letting $\rho_s(\mathbf{r})$ denote the spatially dependent ambient density and $\rho'(\mathbf{r},t)$ denote the linear acoustic perturbation density. Pierce provides the appropriate equation of state:[38]

> If the ambient state is inhomogeneous, $p = p(\rho, s_0)$ cannot be used and one falls back on $p = p(\rho, s)$, $Ds/Dt = 0$ as a starting point. If $p_0(\mathbf{x})$ and $\rho_0(\mathbf{x})$ are independent of t, these lead to
>
> $$\frac{\partial p'}{\partial t} + \mathbf{v}' \cdot \nabla p_0 = c^2\left(\frac{\partial \rho'}{\partial t} + \mathbf{v}' \cdot \nabla \rho_0\right)$$
>
> as the linear equation that replaces $[p' = c^2\rho', c^2 = (\partial p/\partial \rho)_0]$.

Using the notation of the present work, noting that p_0 is a constant and therefore $\nabla p_0 = \mathbf{0}$, and solving for $\partial \rho'/\partial t$ yields

$$\frac{\partial \rho'}{\partial t} = \frac{1}{c^2}\frac{\partial p}{\partial t} - \mathbf{u} \cdot \nabla \rho_s(\mathbf{r}). \tag{B1}$$

Equation (B1) will be used to eliminate the perturbation density from the systems of partial differential equations that follow.

The exact mass conservation equation in an inhomogeneous medium is

$$\frac{\partial}{\partial t}\left[\rho_s(\mathbf{r}) + \rho'(\mathbf{r},t)\right] + \nabla \cdot \left\{\left[\rho_s(\mathbf{r}) + \rho'(\mathbf{r},t)\right]\mathbf{u}\right\} = 0.$$

Neglecting the nonlinear term $\rho'(\mathbf{r},t)\mathbf{u}$ and expanding the divergence of the product $\rho_s(\mathbf{r})\mathbf{u}$ yields

$$\frac{\partial \rho'(\mathbf{r},t)}{\partial t} + \rho_s(\mathbf{r})\nabla \cdot \mathbf{u} + \mathbf{u} \cdot \nabla \rho_s(\mathbf{r}) = 0.$$

Inserting the linearized state equation given by Eq. (B1) and noting that the $\mathbf{u} \cdot \nabla \rho_s(\mathbf{r})$ terms cancel results in

$$\nabla \cdot \mathbf{u} = -\beta_s(\mathbf{r})\frac{\partial p}{\partial t}. \tag{B2}$$

Meanwhile, conservation of momentum requires that

$$\nabla p + \frac{\partial}{\partial t}\left\{\left[\rho_s(\mathbf{r}) + \rho'(\mathbf{r},t)\right]\mathbf{u}\right\} = 0.$$

Neglecting the nonlinear term $\rho'\mathbf{u}$, noting that ρ_s is not a function of time, and solving for $\partial \mathbf{u}/\partial t$ yields

$$\frac{\partial \mathbf{u}}{\partial t} = -\frac{1}{\rho_s(\mathbf{r})}\nabla p. \tag{B3}$$

The wave equation for an inhomogeneous medium is derived by taking the time derivative of Eq. (B2) and the divergence of Eq. (B3). Subtracting the resulting equations yields

$$\nabla \cdot \left[\frac{\nabla p}{\rho_s(\mathbf{r})}\right] = \beta_s(\mathbf{r})\frac{\partial^2 p}{\partial t^2}. \tag{B4}$$

Equation (B4) can be written in terms of the ambient density ρ_0 and compressibility β_0 as

$$\nabla \cdot \left[\left(\frac{1}{\rho_s(\mathbf{r})} - \frac{1}{\rho_0}\right)\nabla p + \frac{\nabla p}{\rho_0}\right] = [\beta_s(\mathbf{r}) - \beta_0]\frac{\partial^2 p}{\partial t^2} + \beta_0\frac{\partial^2 p}{\partial t^2},$$

rearrangement of which yields

$$\nabla^2 p - \beta_0\rho_0\frac{\partial^2 p}{\partial t^2} = -\beta_0\rho_0\left[1 - \frac{\beta_s(\mathbf{r})}{\beta_0}\right]\frac{\partial^2 p}{\partial t^2} - \nabla \cdot \left\{\left[\frac{\rho_0}{\rho_s(\mathbf{r})} - 1\right]\nabla p\right\}. \tag{B5}$$

In terms of the sound speed c_0 and Eq. (4), Eq. (B5) becomes

$$\nabla^2 p - \frac{1}{c_0^2}\frac{\partial^2 p}{\partial t^2} = \frac{\gamma_\beta(\mathbf{r})}{c_0^2}\frac{\partial^2 p}{\partial t^2} + \nabla \cdot \left[\gamma_\rho(\mathbf{r})\nabla p\right]. \tag{B6}$$

Equation (B6) recovers Morse and Ingard's Eq. (8.1.11) for material contrast factors that are not functions of time.[40] Assuming a time-harmonic solution $p(\mathbf{r},t)=\mathrm{Re}[\tilde{p}(\mathbf{r})e^{-i\omega t}]$ reduces Eq. (B6) to Eq. (2), which can be expressed as

$$\nabla^2\tilde{p}+k^2\tilde{p}=-h(\mathbf{r}), \tag{B7}$$

where

$$h(\mathbf{r})=k^2\gamma_\beta\tilde{p}-\boldsymbol{\nabla}\cdot(\gamma_\rho\boldsymbol{\nabla}\tilde{p}). \tag{B8}$$

The particular solution of the inhomogeneous Helmholtz equation is the Helmholtz–Kirchhoff integral given by Morse and Ingard's Eq. (7.1.17),[40]

$$\tilde{p}(\mathbf{r})=\int h(\mathbf{r}_\mathrm{s})G(\mathbf{r}|\mathbf{r}_\mathrm{s})\mathrm{d}V_\mathrm{s}+\oint\left[G(\mathbf{r}|\mathbf{r}_\mathrm{s})\frac{\partial\tilde{p}(\mathbf{r}_\mathrm{s})}{\partial n_\mathrm{s}}-\tilde{p}(\mathbf{r}_\mathrm{s})\frac{\partial G(\mathbf{r}|\mathbf{r}_\mathrm{s})}{\partial n_\mathrm{s}}\right]\mathrm{d}A_\mathrm{s}, \tag{B9}$$

where $G(\mathbf{r}|\mathbf{r}_\mathrm{s})$ is the appropriate Green's function, $\mathbf{r}_\mathrm{s}$ is the spatial integration coordinate, and n_s denotes the normal component of the gradient operator $\boldsymbol{\nabla}_\mathrm{s}$. The volume integral in Eq. (B9) is taken "over the whole volume occupied by the medium," and the surface integral is evaluated "on the surface bounding the medium."[40] Assuming that the volume occupied by the medium is unbounded reduces $G(\mathbf{r}|\mathbf{r}_\mathrm{s})$ to the free-space Green's function given by Eq. (7), and the solution of Eq. (B7) in terms of Eq. (B8) is

$$\tilde{p}(\mathbf{r})=\tilde{p}(\mathbf{r}\to\infty)+\int h(\mathbf{r}_\mathrm{s})g(\mathbf{r}|\mathbf{r}_\mathrm{s})\mathrm{d}V_\mathrm{s}, \tag{B10}$$

where

$$\tilde{p}(\mathbf{r}\to\infty)=\oint\left[g(\mathbf{r}|\mathbf{r}_\mathrm{s})\frac{\partial\tilde{p}(\mathbf{r}_\mathrm{s})}{\partial n_\mathrm{s}}-\tilde{p}(\mathbf{r}_\mathrm{s})\frac{\partial g(\mathbf{r}|\mathbf{r}_\mathrm{s})}{\partial n_\mathrm{s}}\right]\mathrm{d}A_\mathrm{s}.$$

The pressure field infinitely far away from the scatterer is simply the field because of the incident wave $\tilde{p}_\mathrm{i}(\mathbf{r})$, so $\tilde{p}(\mathbf{r}\to\infty)=\tilde{p}_\mathrm{i}(\mathbf{r})$. The total field given by Eq. (B10) is thus represented by Eq. (5), where the second term of Eq. (B10) is interpreted as the scattered wave:

$$\tilde{p}_\mathrm{s}(\mathbf{r})=\int\left\{k^2\gamma_\beta(\mathbf{r}_\mathrm{s})p(\mathbf{r}_\mathrm{s})-\boldsymbol{\nabla}_\mathrm{s}\cdot\left[\gamma_\rho(\mathbf{r}_\mathrm{s})\boldsymbol{\nabla}_\mathrm{s}p(\mathbf{r}_\mathrm{s})\right]\right\}g(\mathbf{r}|\mathbf{r}_\mathrm{s})\,\mathrm{d}V_\mathrm{s}. \tag{B11}$$

Noting from the product rule of divergences that

$$\boldsymbol{\nabla}_\mathrm{s}\cdot\left[\gamma_\rho(\mathbf{r}_\mathrm{s})\boldsymbol{\nabla}_\mathrm{s}\tilde{p}(\mathbf{r}_\mathrm{s})\right]g(\mathbf{r}_\mathrm{s}|\mathbf{r}_\mathrm{s})=\boldsymbol{\nabla}_\mathrm{s}\cdot\left\{\gamma_\rho(\mathbf{r}_\mathrm{s})[\boldsymbol{\nabla}_\mathrm{s}\tilde{p}(\mathbf{r}_\mathrm{s})]g(\mathbf{r}|\mathbf{r}_\mathrm{s})\right\}-\gamma_\rho(\mathbf{r}_\mathrm{s})\boldsymbol{\nabla}_\mathrm{s}\tilde{p}(\mathbf{r}_\mathrm{s})\cdot\boldsymbol{\nabla}_\mathrm{s}g(\mathbf{r}|\mathbf{r}_\mathrm{s}) \tag{B12}$$

allows Eq. (B11) to be written as

$$\tilde{p}_\mathrm{s}(\mathbf{r})=\int k^2\gamma_\beta(\mathbf{r}_\mathrm{s})\tilde{p}(\mathbf{r}_\mathrm{s})g(\mathbf{r}|\mathbf{r}_\mathrm{s})\,\mathrm{d}V_\mathrm{s}-\int\boldsymbol{\nabla}_\mathrm{s}\cdot\left\{\gamma_\rho(\mathbf{r}_\mathrm{s})[\boldsymbol{\nabla}_\mathrm{s}\tilde{p}(\mathbf{r}_\mathrm{s})]g(\mathbf{r}|\mathbf{r}_\mathrm{s})\right\}\mathrm{d}V_\mathrm{s}+\int\gamma_\rho(\mathbf{r}_\mathrm{s})\boldsymbol{\nabla}_\mathrm{s}\tilde{p}(\mathbf{r}_\mathrm{s})\cdot\boldsymbol{\nabla}_\mathrm{s}g(\mathbf{r}|\mathbf{r}_\mathrm{s})\,\mathrm{d}V_\mathrm{s}. \tag{B13}$$

Invoking the divergence theorem allows the second term of Eq. (B13) to be written as

$$-\int\boldsymbol{\nabla}_\mathrm{s}\cdot\left\{\gamma_\rho(\mathbf{r}_\mathrm{s})[\boldsymbol{\nabla}_\mathrm{s}\tilde{p}(\mathbf{r}_\mathrm{s})]g(\mathbf{r}|\mathbf{r}_\mathrm{s})\right\}\mathrm{d}V_\mathrm{s}=-\oint\gamma_\rho(\mathbf{r}_\mathrm{s})\frac{\partial\tilde{p}}{\partial n_\mathrm{s}}g(\mathbf{r}|\mathbf{r}_\mathrm{s})\,\mathrm{d}S_\mathrm{s},$$

which vanishes on the surface at ∞ because $\gamma_\rho=0$ at ∞. The first and third terms of Eq. (B13) therefore yield Eq. (6).

APPENDIX C: DIPOLE-ORDER EXPANSION

The dipole-order expansion of the scattered pressure given by Eq. (17) is derived from first principles by obtaining expressions for volume and force sources, replacing the integrand in Eq. (6) with those expressions, and representing an extended scatterer as a point scatterer.

Consider a sphere centered at the origin whose boundary of radius a pulsates radially with time-harmonic velocity amplitude u_0. The general form of the radiated pressure field is[67]

$$\tilde{p}(r)=B\frac{e^{ikr}}{r}, \tag{C1}$$

where the constant B is determined by substituting Eq. (C1) into the linearized momentum equation $\partial\tilde{p}/\partial r=-i\omega\rho_0u_0$ evaluated at $r=a$:

$$B=-\frac{ika^2\rho_0c_0u_0}{1-ika}e^{-ika}. \tag{C2}$$

Combining Eqs. (C1) and (C2) and assuming $ka\ll1$ yields

$$\tilde{p}(r)=-ik\rho_0c_0Q\frac{e^{ikr}}{4\pi r}, \tag{C3}$$

where $Q=4\pi a^2u_0$ is the volume velocity. If the center of the sphere is translated from the origin $\mathbf{0}$ to another location $\mathbf{r}_\mathrm{s}$, then r in Eq. (C3) is replaced with $R=|\mathbf{r}-\mathbf{r}_\mathrm{s}|$. In view of the free-space Green's function given by Eq. (7), the pressure field due to a monopole at $\mathbf{r}=\mathbf{r}_\mathrm{s}$ can be expressed as

$$\tilde{p}(\mathbf{r}|\mathbf{r}_\mathrm{s})=-ik\rho_0c_0Qg(\mathbf{r}|\mathbf{r}_\mathrm{s}), \tag{C4}$$

recovering the second of Pierce's Eqs. (4-3.1), where it is noted that Pierce's "monopole amplitude" $\hat{S}$ equals $-ik\rho_0c_0\hat{Q}_s/4\pi$.[38]

https://doi.org/10.1121/10.0043002

The field radiated by a dipole is described by two out-of-phase monopoles separated along the z axis by a distance h as

$$\tilde{p}(\mathbf{r}) = -ik\rho_0 c_0 Q[g(\mathbf{r}|z_s = h/2) - g(\mathbf{r}|z_s = -h/2)]. \quad \text{(C5)}$$

In the limit $h \to 0$, Eq. (C5) becomes

$$\tilde{p}(\mathbf{r}) = \rho_0 \dot{Q} h[\partial g/\partial z_s]_{r_s=0}, \quad \text{(C6)}$$

where $\dot{Q} = -ikc_0 Q$ is the time derivative of the volume velocity. Following Blackstock's discussion on p. 369 of Ref. 67, the quantity $\rho_0 \dot{Q} h$ is identified as a time harmonic force F exerted in the z direction. If the separation between the monopoles in Eq. (C5) is not restricted to the z axis and is instead denoted by a separation vector $\mathbf{h}$ extending from the negative monopole to the positive monopole defining the dipole, then the partial derivative of the Green's function with respect to z in Eq. (C6) generalizes to the gradient of the Green's function with respect to $\mathbf{r}_s$. Equation (C6) then becomes

$$\tilde{p}(\mathbf{r}|\mathbf{r}_s) = \mathbf{F} \cdot \nabla_s g(\mathbf{r}|\mathbf{r}_s), \quad \text{(C7)}$$

where $\mathbf{F} = \rho_0 \dot{Q} \mathbf{h}$. Equation (C7) recovers Pierce's Eq. (4-4.1),[38] where the identification of the force vector recovers Pierce's discussion on p. 167 of Ref. 38, in which $\mathbf{F} = -ik\rho_0 c_0 4\pi a^2 u_0 \mathbf{h} = \rho_0 \dot{Q} \mathbf{h}$. In Pierce's notation, the identification is expressed as $\mathbf{F} = 4\pi \hat{\mathbf{d}} = 4\pi \hat{S} \mathbf{d}$, where $\hat{S}$ is the "monopole amplitude" defined on p. 160 for a point source as $-i\omega\rho a^2 \hat{v}_s$.

The integrand of Eq. (6) can be interpreted as the contribution of volume and force sources given by Eqs. (C4) and (C7), respectively. Setting $k^2 \gamma_\beta p \Delta V = -ik\rho_0 c_0 Q$ and $\gamma_\rho \nabla p \Delta V = \mathbf{F}$ yields the identifications

$$q(\mathbf{r}) = \frac{Q}{\Delta V} = \frac{ik}{\rho_0 c_0} \gamma_\beta(\mathbf{r}) \tilde{p}(\mathbf{r}), \quad \text{(C8)}$$

$$\mathbf{f}(\mathbf{r}) = \frac{\mathbf{F}}{\Delta V} = \gamma_\rho(\mathbf{r}) \nabla \tilde{p}(\mathbf{r}). \quad \text{(C9)}$$

In terms of Eqs. (C8) and (C9), Eq. (6) can be expressed as

$$\tilde{p}_s(\mathbf{r}) = -ik\rho_0 c_0 \int q(\mathbf{r}_s) g(\mathbf{r}|\mathbf{r}_s) dV_s + \int \mathbf{f}(\mathbf{r}_s) \cdot \nabla_s g(\mathbf{r}|\mathbf{r}_s) dV_s. \quad \text{(C10)}$$

Equation (C10) recovers the second of Eqs. (A2) of Sieck *et al.*[55] upon replacing kc_0 with ω and noting that the gradient in Eq. (C10) is evaluated over the scatterer's coordinates $\mathbf{r}_s$. The evaluation by Sieck *et al.* of the gradient over the field coordinate $\mathbf{r}$ causes the second term of the second of Eqs. (A2) of Ref. 55 to differ in sign from the second term of Eq. (C10).

The field at $\mathbf{r}$ due to a point scatterer located at the origin $\mathbf{0}$ is obtained by letting $q = -ikc_0 m\delta(\mathbf{r}_s)$ and $\mathbf{f} = ikc_0 \mathbf{d}(\mathbf{r}_s)\delta(\mathbf{r}_s)$ in Eq. (C10), where these definitions are identical to those introduced by Sieck *et al.* on p. 18 of Ref. 55 as

$$\tilde{p}_s(\mathbf{r}) = ik\rho_0 c_0 \int ikc_0 m\delta(\mathbf{r}_s) g(\mathbf{r}|\mathbf{r}_s) dV_s + ikc_0 \int \mathbf{d}(\mathbf{r}_s)\delta(\mathbf{r}_s) \cdot \nabla_s g(\mathbf{r}|\mathbf{r}_s) dV_s. \quad \text{(C11)}$$

Using the sifting property of the delta function yields Eq. (17), which recovers the second of Eqs. (19) of Sieck *et al.*[55] The second term of Eq. (17) differs in sign from the dipole term of the second of Eqs. (19) of Ref. 55 because of the choice of coordinate with respect to which the gradient is evaluated, as illustrated by Pierce's Eq. (4-4.2).[38]

[1] G. R. Torr, "The acoustic radiation force," Am. J. Phys. **52**, 402–408 (1984).
[2] L. P. Gor'kov, "On the forces acting on a small particle in an acoustical field in an ideal fluid," Sov. Phys. Dokl. **6**, 773–775 (1962), Eqs. (8′), (9), and (10).
[3] F. Mignard, "On the radiation forces," in *Interrelations Between Physics and Dynamics for Minor Bodies in the Solar System*, edited by D. Benest and Claude Froeschle (Editions Frontières, Gif-sur-Yvette, France, 1992), pp. 419–451.
[4] J. Needham and C. A. Ronan, *The Shorter Science and Civilisation in China* (Cambridge University Press, Cambridge, UK, 1978), Vol. 2.
[5] J. R. Christianson, "Tycho Brahe's German treatise on the Comet of 1577: A study in science and politics," Isis **70**, 110–140 (1979).
[6] D. Seargent, *The Greatest Comets in History: Broom Stars and Celestial Scimitars* (Springer, New York, 2009), p. 104.
[7] A. Koestler, *The Sleepwalkers: A History of Man's Changing Vision of the Universe* (Hutchinson, London, UK, 1959), p. 232.
[8] J. Kepler, *De Cometis Libelli Tres* (*Three Booklets on Comets*) (A. Apergeri: Avgvstae Vindelicorvum, Augsburg, Germany, 1619).
[9] J. Dalibard, "Atoms and radiation," Lett. Coll. France **8**, 10 (2014).
[10] R. T. Beyer, "Radiation pressure—the history of a mislabeled tensor," J. Acoust. Soc. Am. **63**, 1025–1030 (1978).
[11] J. C. Maxwell, *A Treatise on Electricity and Magnetism* (Clarendon Press, Oxford, UK, 1873).
[12] J. H. Poynting, "Radiation pressure," Philos. Mag. **9**, 393–406 (1905).
[13] J. H. Poynting, "The wave motion of a revolving shaft, and a suggestion as to the angular momentum in a beam of circularly polarised light," Proc. R. Soc. London, Ser. A **82**, 560–567 (1909).
[14] Lord Rayleigh, "On the momentum and pressure of gaseous vibrations, and on the connection with the virial theorem," Philos. Mag. **10**, 364–374 (1905).
[15] A. Kundt, "Über eine neue Art akustischer Staubfiguren und über die Anwendung derselben zur Bestimmung der Schallgeschwindigkeit in festen körpern und Gasen" ("On a new type of acoustic dust figures and on their application for determining the speed of sound in solids and gases"), Ann. Phys. **203**, 497–523 (1866).
[16] Lord Rayleigh, "On the pressure of vibrations," Philos. Mag. **3**, 338–346 (1902).
[17] L. Brillouin, "On radiation stresses," Ann. Phys. **4**, 528–586 (1925).
[18] H. Bruus, "Acoustic radiation force on small particles," in *Microscale Acoustofluidics*, edited by T. Laurell and A. Lenshof (Royal Society of Chemistry, Cambridge, UK, 2014), Sec. 4.3.1.
[19] P. L. Marston and D. B. Thiessen, "Manipulation of fluid objects with acoustic radiation pressure," Ann. N.Y. Acad. Sci. **1027**, 414–434 (2004).
[20] J. Rufo, F. Cai, J. Friend, M. Wiklund, and T. J. Huang, "Acoustofluidics for biomedical applications," Nat. Rev. Methods Primers **2**, 30 (2022).
[21] S. Yang, J. Rufo, Y. Chen, C. Chen, B. W. Drinkwater, L. P. Lee, and T. J. Huang, "Acoustic tweezers for advancing precision biology and medicine," Nat. Rev. Methods Primers **5**, 49 (2025).
[22] P. Mishra, P. Glynne-Jones, R. J. Boltryk, and M. Hill, "Efficient finite element modeling of acoustic radiation forces on inhomogeneous elastic particles," AIP Conf. Proc. **1433**, 753–756 (2012).
[23] T. S. Jerome, Yu. A. Ilinskii, E. A. Zabolotskaya, and M. F. Hamilton, "Born approximation of acoustic radiation force and torque on soft objects of arbitrary shape," J. Acoust. Soc. Am. **145**, 36–44 (2019), Eqs. (3) and (7). Figure 1(a) shows that the Born approximation accurately

predicts the radiation force at $ka = O(10)$ for $\Delta_K = (K_s - K_0)/K_0 = 0.05$, where K_s and K_0 are is the bulk moduli of the scatterer and background medium, respectively.
[24]E. B. Lima and G. T. Silva, "Mean acoustic fields exerted on a subwavelength axisymmetric particle," J. Acoust. Soc. Am. **150**, 376–384 (2021).
[25]R. M. Abraham-Ekeroth, M. Lester, and D. Torrent, "Control and sorting of inhomogeneous dielectric core–shell nanoparticles using two counter-propagating plane waves," Eur. Phys. J. Plus **140**, 123 (2025).
[26]T. S. Jerome, Yu. A. Ilinskii, E. A. Zabolotskaya, and M. F. Hamilton, "Acoustic radiation force on a compressible spheroid," J. Acoust. Soc. Am. **148**, 2403–2415 (2020).
[27]T. S. Jerome and M. F. Hamilton, "Born approximation of acoustic radiation force and torque on inhomogeneous objects," J. Acoust. Soc. Am. **150**, 3417–3427 (2021).
[28]G. Destgeer, B. H. Ha, J. H. Jung, and H. J. Sung, "Submicron separation of microspheres via travelling surface acoustic waves," Lab Chip **14**, 4665–4672 (2014).
[29]Z. Ma, D. J. Collins, J. Guo, and Y. Ai, "Mechanical properties based particle separation via traveling surface acoustic wave," Anal. Chem. **88**, 11844–11851 (2016).
[30]T. J. Matula, O. A. Sapozhnikov, L. A. Ostrovsky, A. A. Brayman, J. Kucewicz, B. E. MacConaghy, and D. D. Raad, "Ultrasound-based cell sorting with microbubbles: A feasibility study," J. Acoust. Soc. Am. **144**, 41–52 (2018).
[31]K. Mutafopulos, P. Spink, C. D. Lofstrom, P. J. Lu, H. Lu, J. C. Sharpe, T. Franke, and D. A. Weitz, "Traveling surface acoustic wave (TSAW) microfluidic fluorescence activated cell sorter (μFACS)," Lab Chip **19**, 2435–2443 (2019).
[32]D. Zhang and C. Ma, "Acoustic metamaterials for remote manipulation of large objects in water," Mater. Horiz. **12**, 4639–4647 (2025).
[33]A. A. Doinikov, "Acoustic radiation forces: Classical theory and recent advances," Recent Res. Dev. Acoust **1**, 39–67 (2003).
[34]B. W. Drinkwater, "A perspective on acoustical tweezers—devices, forces, and biomedical applications," Appl. Phys. Lett. **117**, 180501 (2020), Fig. 1.
[35]M. Smagin, I. Toftul, K. Y. Bliokh, and M. Petrov, "Acoustic lateral recoil force and stable lift of anisotropic particles," Phys. Rev. Appl. **22**, 064041 (2024).
[36]T. Tang and L. Huang, "An efficient semi-analytical procedure to calculate acoustic radiation force and torque for axisymmetric irregular bodies," J. Sound Vib. **532**, 117012 (2022).
[37]T. Tang, Y. Zhang, B. Dong, and L. Huang, "Computation of acoustic scattered fields and derived radiation force and torque for axisymmetric objects at arbitrary orientations," J. Acoust. Soc. Am. **156**, 2767–2782 (2024).
[38]A. D. Pierce, *Acoustics: An Introduction to Its Physical Principles and Applications*, 2nd ed. (Acoustical Society of America, Woodbury, NY, 1989), Eqs. (1-11.2)–(1-11.4), and (1-11.10a), Sec. 1-5, pp. 153–170, 431–433, 441–443.
[39]H. C. van de Hulst, *Light Scattering by Small Particles* (Wiley, New York, 1957), pp. 13–14, 63–65, 75, 85.
[40]P. M. Morse and K. U. Ingard, *Theoretical Acoustics* (McGraw-Hill, New York, 1968), Eqs. (8.1.11)–(8.1.15), (8.1.20), (8.1.21), and (8.2.3), pp. 407–414. The contrast factor γ_κ is equivalent to γ_β used in the present work. The second term on the right-hand side of Eq. (8.1.12) should be added to, not subtracted from, the equation.
[41]M. I. Mishchenko, W. J. Wiscombe, J. W. Hovenier, and L. D. Travis, "Overview of scattering by nonspherical particles," in *Light Scattering by Nonspherical Particles: Theory, Measurements, and Applications*, edited by M. I. Mishchenko, J. W. Hovenier, and L. D. Travis (Academic Press, San Diego, CA, 2000), Chap. 1, pp. 45–48.
[42]P. J. Westervelt, "The theory of steady forces caused by sound waves," J. Acoust. Soc. Am. **23**, 312–315 (1951), Eq. (8).
[43]P. J. Westervelt, "Acoustic radiation pressure," J. Acoust. Soc. Am. **29**, 26–29 (1957), Eqs. (4), (8), (12), and (16), Footnote 2.
[44]L. Zhang and P. L. Marston, "Geometrical interpretation of negative radiation forces of acoustical Bessel beams on spheres," Phys. Rev. E **84**, 035601 (2011), Eq. (21).
[45]L. Zhang and P. L. Marston, "Acoustic radiation force expressed using complex phase shifts and momentum-transfer cross sections," J. Acoust. Soc. Am. **140**, EL178–EL183 (2016).
[46]J. H. Ginsberg, *Acoustics: A Textbook for Engineers and Physicists* (Springer, Cham, Switzerland, 2018), Vol. 2, Eqs. (7.4.23) and (7.4.31), pp. 100, 490–504.
[47]R. Löfstedt and S. Putterman, "Theory of long wavelength acoustic radiation pressure," J. Acoust. Soc. Am. **90**, 2027–2033 (1991).
[48]L. Zhang and P. L. Marston, "Acoustic radiation torque and the conservation of angular momentum (L)," J. Acoust. Soc. Am. **129**, 1679–1680 (2011).
[49]P. L. Marston, S. G. Goosby, D. S. Langley, and S. E. LoPorto-Arione, "Resonances, radiation pressure and optical scattering phenomena of drops and bubbles," in *Proceedings of the Second International Colloquium on Drops and Bubbles*, NASA, Jet Propulsion Lab, California Institute of Technology, Pasadena, CA (November 19–21, 1981) (1982), pp. 166–174.
[50]T. Leighton, *The Acoustic Bubble* (Academic Press, London, UK, 1994).
[51]L. Ostrovsky, "Concentration of microparticles and bubbles in standing waves," J. Acoust. Soc. Am. **138**, 3607–3612 (2015).
[52]O. A. Sapozhnikov and M. R. Bailey, "Radiation force of an arbitrary acoustic beam on an elastic sphere in a fluid," J. Acoust. Soc. Am. **133**, 661–676 (2013), Eq. (17).
[53]D. L. Colton and R. Kress, *Inverse Acoustic and Electromagnetic Scattering Theory*, 4th ed. (Springer, Cham, Switzerland, (2019), pp. 440–441.
[54]S. Moskow and J. C. Schotland, "Convergence and stability of the inverse scattering series for diffuse waves," Inverse Probl. **24**, 065005 (2008).
[55]C. F. Sieck, A. Alù, and M. R. Haberman, "Origins of Willis coupling and acoustic bianisotropy in acoustic metamaterials through source-driven homogenization," Phys. Rev. B **96**, 104303 (2017), Eqs. (16), (32), (40), and (A2).
[56]X. Su and A. N. Norris, "Retrieval method for the bianisotropic polarizability tensor of Willis acoustic scatterers," Phys. Rev. B **98**, 174305 (2018), Eqs. (1) and (16).
[57]L. Quan, Y. Ra'di, D. L. Sounas, and A. Alù, "Maximum Willis coupling in acoustic scatterers," Phys. Rev. Lett. **120**, 254301 (2018), Eqs. (5), (S23), (S32), and (S33).
[58]X.-D. Fan and L. Zhang, "Phase shift approach for engineering desired radiation force: Acoustic pulling force example," J. Acoust. Soc. Am. **150**, 102–110 (2021), Figs. 3(a) and 3(b).
[59]S. Sepehrirahnama, S. Oberst, Y. K. Chiang, and D. A. Powell, "Acoustic radiation force and radiation torque beyond particles: Effects of nonspherical shape and Willis coupling," Phys. Rev. E **104**, 065003 (2021), Eqs. (5) and (7).
[60]S. Sepehrirahnama and S. Oberst, "Acoustic radiation force and torque acting on asymmetric objects in acoustic Bessel beam of zeroth order within Rayleigh scattering limit," Front. Phys. **10**, 897648 (2022).
[61]S. Sepehrirahnama, S. Oberst, Y. K. Chiang, and D. A. Powell, "Willis coupling-induced acoustic radiation force and torque reversal," Phys. Rev. Lett. **129**, 174501 (2022).
[62]R. P. Feynman, *Feynman Lectures on Physics* (Basic Books, New York, 2013), Vol. II, Chap. 31, https://www.feynmanlectures.caltech.edu/III_copyright.html for more information.
[63]D. J. Griffiths, *Introduction to Electrodynamics*, 3rd ed. (Pearson, Upper Saddle River, NJ, 1999), pp. 39, 161–163. See inside back cover for conversions between Cartesian and spherical unit vectors.
[64]A. Alù, "First-principles homogenization theory for periodic metamaterials," Phys. Rev. B **84**, 075153 (2011), Eq. (16).
[65]T. B. A. Senior, "Low-frequency scattering," J. Acoust. Soc. Am. **53**, 742–747 (1973).
[66]A. J. Lawrence, "On acoustic multiple scattering from Willis media," Ph.D. dissertation, University of Texas at Austin, Austin, TX, 2024, pp. 38–45.
[67]D. T. Blackstock, *Fundamentals of Physical Acoustics* (Wiley, New York, 2000), Eqs (1.D-16), (1.E-12a), (1.E-18d), (11.A-14), (11.A-36), and (12.B-10), Table 11.1, pp. 44 and 360.
[68]Lord Rayleigh, "On the scattering of light by small particles," Philos. Mag. **41**, 375–384 (1871).
[69]Lord Rayleigh, "Investigation of the disturbance produced by a spherical obstacle on the waves of sound," Proc. London Math. Soc. **4**, 253–283 (1872).
[70]Lord Rayleigh, "On the light from the sky, its polarization and colour," Philos. Mag. **41**, 107–120 (1871).

[71]P. L. Marston, "Phase-shift derivation of expansions for material and frequency dependence of progressive-wave radiation forces and backscattering by spheres," J. Acoust. Soc. Am. **145**, EL39–EL44 (2019).
[72]P. L. Marston, "Finite-size radiation force correction for inviscid spheres in standing waves," J. Acoust. Soc. Am. **142**, 1167–1170 (2017).
[73]P. L. Marston, "Contrast factor for standing-wave radiation forces on spheres: Series expansion in powers of sphere radius," JASA Express Lett. **4**, 074001 (2024).
[74]P. L. Marston and L. Zhang, "Relationship of scattering phase shifts to special radiation force conditions for spheres in axisymmetric wavefields," J. Acoust. Soc. Am. **141**, 3042–3049 (2017).
[75]P. L. Marston, "Concentric fluid spheres: Scattering and radiation forces and the lowest monopole resonance of bubble shells," JASA Express Lett. **5**, 094002 (2025).
[76]A. F. Stevenson, "Solution of electromagnetic scattering problems as power series in the ratio (dimension of scatterer)/wavelength," J. Appl. Phys. **24**, 1134–1142 (1953).
[77]P. L. Marston, "Born approximation for scattering by evanescent waves: Comparison with exact scattering by an infinite fluid cylinder," J. Acoust. Soc. Am. **115**, 2473 (2004).
[78]J. B. Keller, R. E. Kleinman, and T. B. A. Senior, "Dipole moments in Rayleigh scattering," IMA J. Appl. Math. **9**, 14–22 (1972).
[79]R. E. Kleinman and T. B. A. Senior, "Rayleigh scattering," in *Low and High Frequency Asymptotics* (Elsevier, Amsterdam, The Netherlands, 1986), Vol. 2, Chap. 1, pp. 2–70.
[80]A. Melnikov, Y. K. Chiang, L. Quan, S. Oberst, A. Alù, S. Marburg, and D. Powell, "Acoustic meta-atom with experimentally verified maximum Willis coupling," Nat. Commun. **10**, 3148 (2019).
[81]L. Quan, S. Yves, Y. Peng, H. Esfahlani, and A. Alù, "Odd Willis coupling induced by broken time-reversal symmetry," Nat. Commun. **12**, 2615 (2021).
[82]P. L. Marston, "Acoustic radiation force and scattering series expansions for spheres at low frequencies," in *Proceedings of the 72nd Annual Meeting of the APS Division of Fluid Dynamics*, American Physical Society, Seattle, WA (November 23–26) (2019), pp. Q06.00001.
[83]M. B. Muhlestein, C. F. Sieck, A. Alù, and M. R. Haberman, "Reciprocity, passivity and causality in Willis materials," Proc. R. Soc. A **472**, 20160604 (2016).
[84]M. B. Muhlestein, C. F. Sieck, P. S. Wilson, and M. R. Haberman, "Experimental evidence of Willis coupling in one-dimensional effective material element," Nat. Commun. **8**, 15625 (2017).
[85]A. Srivastava and S. Nemat-Nasser, "On the limit and applicability of dynamic homogenization," Wave Motion **51**, 1045–1054 (2014), Sec. 3.2.
[86]A. Srivastava, "Elastic metamaterials and dynamic homogenization: A review," Int. J. Smart Nano Mat. **6**, 41–60 (2015).
[87]Y.-Y. Wang, J. Yao, X.-W. Wu, D.-J. Wu, and X.-J. Liu, "Influences of the geometry and acoustic parameter on acoustic radiation forces on three-layered nucleate cells," J. Appl. Phys. **122**, 094902 (2017), Table 1, Eq. (6).
[88]Yu. A. Ilinskii, E. A. Zabolotskaya, B. C. Treweek, and M. F. Hamilton, "Acoustic radiation force on an elastic sphere in a soft elastic medium," J. Acoust. Soc. Am. **144**, 568–576 (2018).
[89]NIST Digital Library of Mathematical Functions, https://dlmf.nist.gov/10.60, Item 10.60.7.
[90]B. C. Treweek, "Acoustic radiation force due to sound beams incident on spherical scatterers in soft tissue-like media," Ph.D. dissertation, University of Texas at Austin, Austin, TX, 2019, Eqs. (3.82) and (3.83).
[91]P. L. Marston, "Axial radiation force of a Bessel beam on a sphere and direction reversal of the force," J. Acoust. Soc. Am. **120**, 3518–3524 (2006), Eq. (13).
[92]P. L. Marston, "Scattering of a Bessel beam by a sphere," J. Acoust. Soc. Am. **121**, 753–758 (2007).
[93]P. L. Marston, T. D. Daniel, A. R. Fortuner, I. P. Kirsteins, and A. T. Abawi, "Specular-reflection contributions to static and dynamic radiation forces on circular cylinders," J. Acoust. Soc. Am. **149**, 3042–3051 (2021), Appendix C.
[94]P. L. Marston, T. D. Daniel, and A. R. Fortuner, "Specular reflection contributions to dynamic radiation forces on highly reflecting spheres (L)," J. Acoust. Soc. Am. **150**, 25–28 (2021), Eq. (4).
[95]P. A. Chinnery, V. F. Humphrey, and J. Zhang, "Low-frequency acoustic scattering by a cube: Experimental measurements and theoretical predictions," J. Acoust. Soc. Am. **101**, 2571–2582 (1997).
[96]D. H. Napper, "A diffraction theory approach to the total scattering by cubes," Kolloid Z. Z. Polym. **218**, 41–46 (1967).
[97]A. Masłowska, P. J. Flatau, and G. L. Stephens, "On the validity of the anomalous diffraction theory to light scattering by cubes," Opt. Commun. **107**, 35–40 (1994).
[98]M. W. Ospel, "Iterative path expansion for Helmholtz scattering with Neumann boundary conditions," J. Acoust. Soc. Am. **159**, 600–609 (2026).
[99]A. Papoulis, *Systems and Transforms with Applications in Optics*, (McGraw-Hill, New York, 1968), Table. 1-1, p. 65.
[100]X. Peng, W. He, F. Xin, G. M. Genin, and T. J. Lu, "Standing surface acoustic waves, and the mechanics of acoustic tweezer manipulation of eukaryotic cells," J. Mech. Phys. Solids **145**, 104134 (2020).
[101]C. A. Gokani, T. S. Jerome, M. R. Haberman, and M. F. Hamilton, "Born approximation of acoustic radiation force used for acoustofluidic separation," Proc. Mtgs. Acoust. **48**, 045002 (2022).
[102]A. Smirnov, S. Chugunov, A. Kholodkova, M. Isachenkov, A. Vasin, and I. Shishkovsky, "Progress and challenges of 3D-printing technologies in the manufacturing of piezoceramics," Ceram. Int. **47**, 10478–10511 (2021).
[103]Y. Harada and T. Asakura, "Radiation forces on a dielectric sphere in the Rayleigh scattering regime," Opt. Commun. **124**, 529–541 (1996), Eq. (12).
[104]X. Fan and L. Zhang, "Born approximation of trapping forces by acoustical Bessel and vortex fields," J. Acoust. Soc. Am. **154**, 3354–3363 (2023).
[105]M. C. Jo and R. Guldiken, "Active density-based separation using standing surface acoustic waves," Sens. Actuators, A **187**, 22–28 (2012).
[106]G. Maidanik, "Torques due to acoustical radiation pressure," J. Acoust. Soc. Am. **30**, 620–623 (1958), Eq. (28).
[107]S. G. Kargl and P. L. Marston, "Ray synthesis of Lamb wave contributions to the total scattering cross section for an elastic spherical shell," J. Acoust. Soc. Am. **88**, 1103–1113 (1990).
[108]P. A. Martin, "On the far-field computation of acoustic radiation forces," J. Acoust. Soc. Am. **142**, 2094–2100 (2017), Eq. (18).
[109]T. Hasegawa, T. Kido, T. Iizuka, and C. Matsuoka, "A general theory of Rayleigh and Langevin radiation pressures," J. Acoust. Soc. Jpn. E. **21**, 145–152 (2000).
[110]T. G. Wang and C. P. Lee, "Radiation pressure and acoustic levitation," in *Nonlinear Acoustics*, 3rd ed., edited by M. F. Hamilton and D. T. Blackstock (Springer, Cham, Switzerland, 2024), Chap. 6, Eqs. (6.7), (6.13), and (6.82), pp. 176–180, 193.
[111]A. A. Doinikov, "Theory of acoustic radiation pressure for actual fluids," Phys. Rev. E **54**, 6297–6303 (1996), Eqs. (4) and (7).
[112]H. Lamb, *Hydrodynamics*, 6th ed. (Dover, New York, 1945), p. 658, Eq. (10).
[113]L. Zhang and P. L. Marston, "Axial radiation force exerted by general non-diffracting beams," J. Acoust. Soc. Am. **131**, EL329–EL335 (2012), Eq. (8).
[114]L. Zhang and P. L. Marston, "Optical theorem for acoustic non-diffracting beams and application to radiation force and torque," Biomed. Opt. Express. **4**, 1610–1617 (2013).
[115]P. L. Marston and L. Zhang, "Unphysical consequences of negative absorbed power in linear passive scattering: Implications for radiation force and torque," J. Acoust. Soc. Am. **139**, 3139–3144 (2016).